FORECASTING PRODUCTION IN UNDEVELOPED, UNCONVENTIONAL PLAYS USING RATE TRANSIENT ANALYSIS AND EXPERIMENTAL DESIGN

A Thesis

by

MORGAN ANNE QUIST

Submitted to the Office of Graduate and Professional Studies of
Texas A&M University
in partial fulfillment of the requirements for the degree of

MASTER OF SCIENCE

Chair of Committee,	W. John Lee
Committee Members,	Duane McVay
	Yuefeng Sun
Head of Department,	Jeff Spath

December 2018

Major Subject: Petroleum Engineering

ABSTRACT

A *complete* inventorying of resources, under the *Petroleum Resources Management System* (PRMS), requires credible low, best, and high case forecasts at all resources classification levels (Reserves, Contingent resources, and Prospective resources). Repeatable and accepted methodology for forecasting production and calculating EURs for each of these classification levels are not available: current methods to forecast production are inadequate for undeveloped resources, as they require production or pressure history, are overly simplified, or are time consuming and financially burdensome. Additionally, these methods do not quantify the level of uncertainty associated with a given forecast, which is needed to comply with the low, best, and high forecasts (often associated with a probability, P10, P50, P90), needed for inventorying under PRMS framework.

RTA has been hailed as a happy medium between empirical and numerical simulation techniques to forecast production in unconventional, undeveloped plays in that it considers the completion and reservoir mechanics of the well and of the formation from which it produces (like numerical simulation techniques, unlike empirical techniques), and is straight-forward and user-friendly (like empirical techniques, unlike numerical simulation techniques). RTA also, does not require production history to generate a production forecast.

However, there are currently few practical methods in industry which allow for the probabilistic forecasting of production using RTA. While we can consider a "best match" (or P50) forecast generated with RTA as a 2P (i.e., best or most likely) forecast,

regulators and investors are far more interested in 1P (lower volume, high confidence) forecasts. The purpose of this work is to develop a workflow to generate a range of production forecasts using RTA techniques, from which probabilistic forecasts can be extracted. The methods involve first history-matching available production data, by varying critical reservoir and completion parameters to find the reservoir and completion parameter combinations which yield a best-fit (via least deviation calculated rate trends from observed rate trends). From this condensed number of best-fit history matches, appropriate probabilistic production forecasts for a certain well can be extrapolated.

In this work, we show that incorporating Experimental Design (ED/DOE) techniques makes RTA a more practical production forecasting technique, reducing the number of history matches that need to be assessed, from which production forecasts can be generated. From this reduced set of best-fit history matches, appropriate probabilistic forecasts and EURs in accordance with PRMS and SEC standards, can be extracted.

DEDICATION

I dedicate this thesis to everyone who has *helped* me:

My family, who has supported me non-stop in pursuing my goals; thank you for giving advice, tough love, and humor when I needed it most. Thank you also, for helping me move across the country two times in less than two years.

My friends, who inspire me to work hard to achieve success, but remind me to have fun. And, to my peers here at Texas A&M for the same reasons: thank you for constantly teaching me new things, and for making the past two years in College Station more fun than I could have ever thought possible. I don't want to know what these past two years looked like without you.

My colleagues and professional network, in the ways you have helped me grow in my career as an engineer, taken a chance on me, taught me new things, or simply emailed me back: thank you. I vow to pay it forward in my career, and extend a helping hand to others when given the opportunity.

Thank you all for the memories and the support – I am very grateful.

ACKNOWLEDGEMENTS

I would like to thank the chair of my committee, Dr. W. John Lee, for devoting his time and for his support throughout the progression of this work. I would also like to thank him not only for his role as my adviser and professor, but also for his role as a professional mentor, for his commitment to industry and life-long learning, and for instilling the value of life-long learning into his students. I am very grateful and humbled to have worked under someone who is so well respected in, and has contributed so much to, this industry.

I also appreciate Dr. Duane McVay and Dr. Yuefeng Sun for giving their time and support to serve as members of my committee. I am very appreciative of you fitting me into your busy schedules!

I also must thank Dr. Akhil Datta-Gupta: had it not been for him, I perhaps would not have pursued this degree, and at this great university.

Thank you also, to the Texas A&M College of Engineering for the generous funding received—as part of the Engineering Graduate Merit Fellowship—to further my education. I am so grateful to have been awarded this fellowship to pursue my degree.

Last, but not least, I owe a special thank you to Mina Moussa and to James Ewart (IHS), both of whom were kind enough to give their time to help me throughout portions of this work.

Thank you!

CONTRIBUTORS AND FUNDING SOURCES

Contributors

This work was supported by a thesis committee consisting of Professor W. John Lee and Duane McVay of the Department of Petroleum Engineering, and Professor Yuefeng Sun of the Department of Geology. All work conducted for the thesis was completed by the student independently.

Funding Sources

This work and graduate study was supported by an Engineering Graduate Merit Fellowship, awarded by the Texas A&M University College of Engineering.

NOMENCLATURE

A_f = Fractured area (ft^2)

B_{gi} = Formation volume factor

b = Arps' b-factor

b' = Intercept of normalized gas pressure vs. $\sqrt{t}$ plot

c_t = Total compressibility (psi^{-1})

c_f = Formation compressibility (psi^{-1})

D_i = Arps' decline parameter, (time-1)

h = Formation thickness (ft)

k = Permeability (nd)

L_{ex} = Lateral length (ft)

$m(p_i)$ = Pseudo-initial pressure

$m(p_{wf})$ = Psedo-flowing well pressure

m_{cp} = Match parameter, and slope of normalized gas pressure vs. $\sqrt{t}$ plot

m_{cpT} = "Target" m_{cp}, and slope of normalized gas pressure vs. $\sqrt{t}$ plot

n_f = Number of fractures

P_{gas} = Gas price ($/Mscf) or ($/MMscf)

p_i = Initial reservoir pressure (psi)

p_{wf} = Flowing well pressure (psi)

q_i = Initial flowrate (MMscf/ time)

q = Production rate (MMscf/ time)

Q = Cumulative production (MMscf)

s = Skin factor, dimensionless

S_g = Gas saturation (%)

S_o = Oil saturation (%)

S_w = Water saturation (%)

t = Time (hours, days, months, years)

t_{elf} = Time to end of linear flow (hours, days, months, years)

x_f = Fracture half-length (ft)

Acronyms

BDF = Boundary-dominated flow

DCA = Decline curve analysis

DOE = Design of Experiments

E&P = Exploration & Production

ED = Experimental Design

EL_{gas} = Economic Limit, gas (MMscf/ month) OR (Mscf/ month)

EUR = Estimated Ultimate Recovery (MMscf)

FCD = Dimensionless fracture conductivity

IRR = Internal rate of return (%)

LOE = Lease Operating Expense ($/well/month)

MCS = Monte Carlo Simulation

MFHW = Multi-fractured horizontal well

NPV = Net present value ($)

NRI = Net Revenue Interest (%)

OGIP = Original gas in place (MMscf)

P10 = Value at confidence level 10%

P50 = Value at confidence level 50%

P90 = Value at confidence level 90%

PRMS = Petroleum Resources Management System

RTA = Rate Transient Analysis

SRV = Stimulated reservoir volume

SSE = Sum of squared errors

TVD = Total vertical depth (ft.)

WI = Working Interest (%)

Greek Nomenclature

Φ = Phi, porosity (%)

μ = Viscosity (cp)

TABLE OF CONTENTS

Page

LIST OF FIGURES

Page

LIST OF TABLES

Page

1. INTRODUCTION

1.1 Background

The development of unconventional plays has revolutionized the oil and gas industry within the United States. Resources from unconventional plays, previously thought to be economically and commercially inaccessible, are now prolific and lucrative. The development of new technologies and completion techniques in recent history (specifically, horizontal drilling and hydraulic fracturing technologies) have positioned the United States as the leading oil and gas producing country in the world, recently surpassing two oil giants (Saudi Arabia and Russia) in annual production rates. **Fig. 1** presents the top six oil producing countries from 1980 to 2017, showing sharp production increase from the United States after 2010, which can be attributed to the "shale boom."

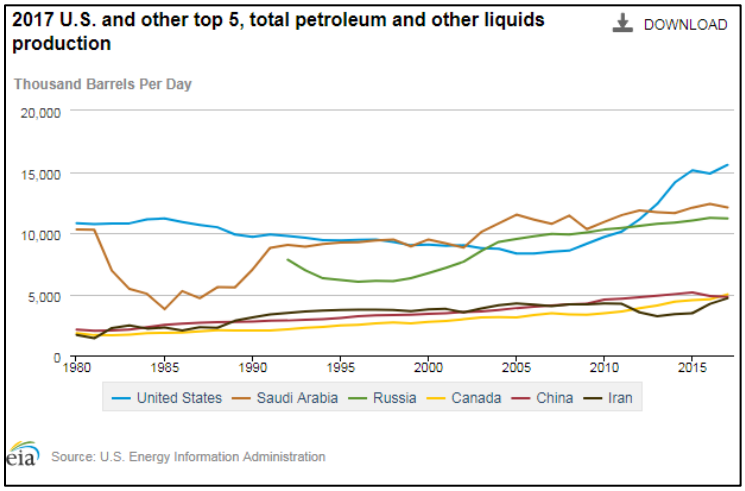

Fig. 1—Top five petroleum (and other liquid) producing countries. Reprinted from the U.S. EIA (2017)

Between 2005 and 2010, the rate at which the United States produced crude oil was on track to match or exceed the rate at which crude oil was produced by Saudi Arabia and Russia, two of the world's long-leading oil and gas giants. Around 2012, U.S. production surpassed all other countries, becoming the world's top oil producing country. (U.S. EIA, 2017).

As of 2015, the United States was also the top natural gas producing country in the world, having produced 27,065 Bcf of natural gas, as shown in **Fig. 2**. Russia closely trailed United States in natural gas production, both countries far surpassing Iran, the world's third top natural gas producing country at that time, which had produced less than 25% of United States production levels in that year (EIA, 2015).

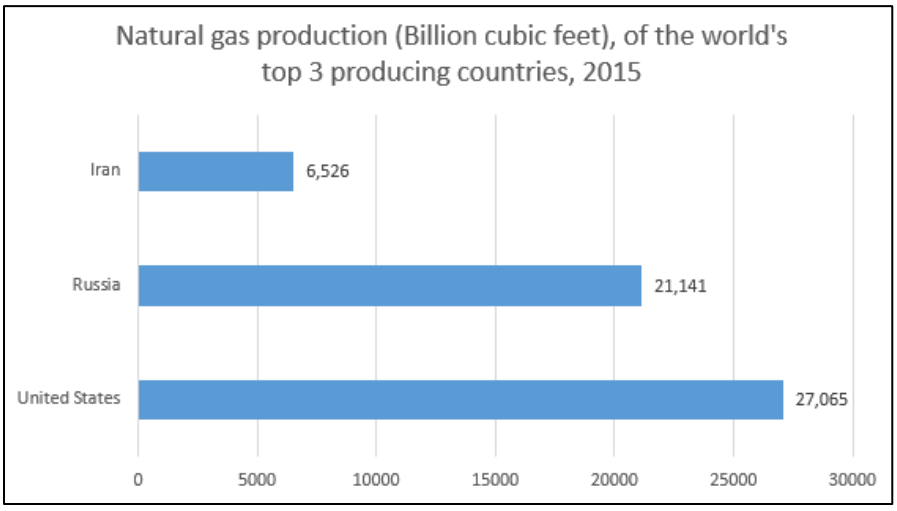

Fig. 2—Top three natural gas producing countries, 2015

Employing these new drilling and completion technologies has not only led to an increase in annual oil and natural gas production within the United States; these technologies have subsequently led to an increase in national reserves: (proved) reserves of crude oil and condensate, as well as natural gas reserves, from 1966-2016 are shown in **Fig. 3**. The large spikes to national reserves observed between 2006 and 2011, can also be attributed to the "shale boom" (U.S. EIA, 2017). As of 2013, the United States has 322.7 trillion cubic feet of gas reserves and 33.4 billion barrels of oil (EIA, 2012-13).

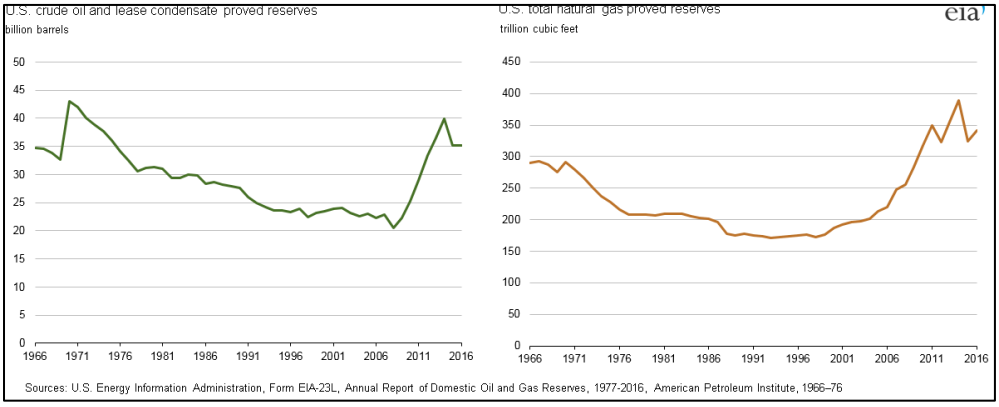

Fig. 3—United States oil and gas proven reserves, 1966-2016. Reprinted from the U.S. EIA (2017)

While there is much opportunity to develop these unconventional plays previously thought to be uneconomic, the geologic complexity of these plays (primarily, the extremely low values of permeability) makes estimating ultimate recovery in these plays (especially on an individual well basis) with high confidence very difficult.

Despite the prolific production and the success of advanced completion technologies in unconventional exploration and production, forecasting production and estimating ultimate recovery in these plays is still widely misunderstood.

There is a considerable amount of uncertainty which currently exists in the oil and gas industry, whether it be estimating geologic parameters, or estimating project costs and revenues, and estimating total recovery estimates in these plays are no exception. Capen (1976) discusses the difficulty of assessing uncertainty, how we as humans tend to be overconfident in estimating a range of potential outcomes, much narrower than what exists in reality. McVay (2015) echoes this, reporting that overconfidence combined with a "directional bias" leads to poor estimates, and that executing plans based on these poor estimates can lead to unfortunate consequences: he notes that over-promising and under-delivering has yielded "portfolio disappointment" for E&P companies, including NPV realizations that are a mere 30%-35% of what is initially estimated in some cases. Quantifying the uncertainty associated with a given EUR or with a given production forecast allows us to make better decisions. In short, Capen (1976) and others in industry have shown that our inabilities to correctly asses a *range* of outcomes can lead to serious financial consequences.

In short, we need to disregard our biases and "guess" better, by *guessing* less, and always have a range of reasonable scenarios to root business planning and development decisions. Especially in the early stages of development, estimating ultimate recovery and, subsequently, making business development plans, is much more difficult for unconventional plays than it is for their conventional, geologically simpler counterparts. While higher uncertainty associated with a forecast in unconventional

plays can be attributed to the geologic complexity, having little to no knowledge of past production only heightens this uncertainty.

1.2 Status of the Question

A *complete* inventorying of resources, under the *Petroleum Resources Management System* (PRMS), requires credible low, best, and high case forecasts and estimates (resources *categories*) at all resources *classification* levels (reserves, contingent resources, and prospective resources). This inventorying system is explained graphically, in the Petroleum Resources Management System (PRMS) Matrix. The PRMS matrix, shown in **Fig. 4,** is complete with "resources classifications" (reserves, contingent resources, and prospective resources), and "resources categories" (level of certainty).

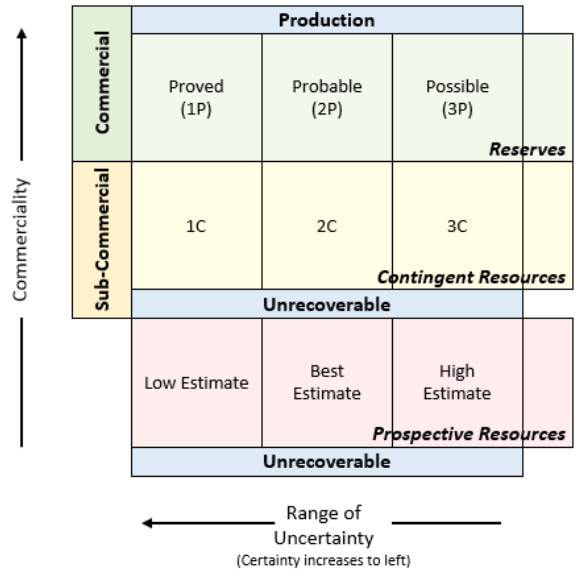

Fig. 4—PRMS resources classification matrix

The PRMS "categories" (horizontal axis) furthest left within each classification (vertical axis) is regarded as the bucket which holds our most conservative recovery estimates (or as the category for the estimates in which we are most confident), while the category furthest right is regarded as the bucket which holds our most optimistic recovery estimates (or as the category where we place estimates in which we are least confident). As our confidence in an estimate increases, our estimate of the recoverable resource volume decreases: the "low" estimate is our highest-confidence estimate (often referred to as the "P90" estimate) and the high estimate is our lowest-confidence estimate (often referred to as the "P10" estimate).

Repeatable, practical, and accepted methodology for forecasting production and calculating EURs at all classification and categorization levels is not available, but needed for unconventional resources, especially for undeveloped—*contingent* and *prospective*—resources. Current methods to do so are time-and money-intensive, are over simplified (and do not consider critical physical components of the reservoir or well), or require historical production rates to extrapolate an outlook for production rates. Probabilistic forecasts for undeveloped resources must be based solely on probability distributions of representative reservoir and completion parameters, since, for these resources classifications, there is no production history to match. This makes estimating production behavior extremely difficult.

There is a need for a methodology in industry which allows us to estimate 1P, 2P, and 3P reserves, as well as 1C, 2C, and 3C contingent resources and "low," "best," and "high" prospective resources in unconventional plays which meet SEC and PRMS

standards. The motivation for this work is to make Rate Transient Analysis (RTA) a more practical method to probabilistically forecast production, and estimate ultimate recovery in undeveloped, unconventional plays. We propose that history-matching limited production data (and subsequently, probabilistically forecasting production) with RTA could be more practical by incorporating Experimental Design (ED, or DOE) techniques. Introducing a practical, and physically sound method to probabilistically forecast production in undeveloped plays is of great value to industry, as assessing a range of scenarios (consistent with regulatory guidelines) of reserves, contingent resources, and prospective resources, is necessary for purposes of reserves disclosures and financial reporting purposes, for regulators and investors. In addition, quality inventorying of resources is integral for operating companies for budget and project planning purposes.

1.3 Objectives and Application

This work delivers a systematic workflow to probabilistically forecast production and estimate ultimate recovery for wells with limited production data using Rate Transient Analysis (RTA) and by incorporating Experimental Design, or Design of Experiments (ED, or DOE), techniques. By incorporating DOE techniques into the process of forecasting production with RTA, the number of forecasts required to form a satisfactory and valid probabilistic range of outcomes is systematically reduced. This subsequently reduces the computational and analysis time required to assemble this range of possible outcomes, which is especially beneficial for project planning in

unconventional plays, as thousands of wells actively continue to be planned and drilled in these plays.

1.4 Current Forecasting Methods

Current methods to probabilistically forecast production are inadequate for undeveloped resources in unconventional plays, as they often require production history, or are overly simplistic, making them unsuitable for capturing the geologic and flow complexities of unconventional plays. Currently available methods to forecast production which *do* have the capacity to capture these complexities, however, are regarded as so detailed and specific that generating large numbers of forecasts to generate a probabilistic *range* of forecasts becomes time-consuming and financially burdensome. These methods also come with a steep learning curve, making them unattractive to a wide audience.

We review some popular methods used to estimate reserves and resources volumes and to forecast production here; the application of these methods is dependent upon the amount of production data available (and whether it is available), on the reservoir and well information available, and on the characterization of the reservoir. We also address the limitations of each method as they relate to estimating ultimate recovery and production forecasting in undeveloped, unconventional plays.

- *Volumetric Analysis.* Volumetric analysis is a simple, physically sound method to estimate reserves and resources volumes; however, this method requires knowledge of recovery factors, and knowledge of parameters used to estimate drainage volume such as formation thickness, drainage area, porosity, initial water saturation,

and initial reservoir pressure. While Monte Carlo Simulation (MCS) and other probabilistic methods could be used to develop a range of possible recovery volumes with volumetric analysis, if the required input parameters are not known accurately, estimated ranges of recovery would be erroneous. Additionally, volumetric analysis does not help us to forecast production in with time. The heterogeneity in unconventional plays also introduces a potential challenge in accurate estimation of volumes in place.

- *Material Balance Analysis (MBA).* Material balance can be used to forecast gas production, and, like volumetric analysis, is simple in application. However, MBA requires average reservoir pressure data to forecast production; when evaluating undeveloped resources plays, this information is unavailable. This method also does not take into consideration many other physical parameters of the reservoir or well

- *Arps' Decline Relations.* Decline curve analysis (DCA), and especially Arps' decline relations, are arguably the most common method used to forecast production in industry today. Arps' decline relations are easy to implement, and require no physical information about the reservoir, or of the well itself, to forecast production. However, the accuracy of these methods are limited, as they are applicable only to wells producing in boundary-dominated flow (BDF). Because unconventional wells do not reach BDF for extended amounts of time—years—sometimes persisting in transient linear flow for the duration of well life, Arps' decline relations are inadequate for forecasting production in unconventional plays, especially during early times of production. Significant advancements have been made in industry in recent years to

develop DCA methods applicable to unconventional shale plays, but they lack a sound fundamental basis.

- *Numerical Simulation.* Advanced techniques such as numerical simulation, can be used to forecast production in unconventional plays for volumes of any resources classification. Numerical simulation techniques require specific physical parameters of the well and reservoir, and are robust tools to forecast production. However, when trying to forecast many wells at one time—or many forecasts in a probabilistic range—numerical simulation techniques become extremely burdensome. Not only does generating a forecast in this way require extended amounts of time due to the amount of computational power used, but it also requires specialized knowledge of the simulation program to work properly. Numerical simulation is considered to be a rigorous approach to generate forecasts, and reserves and resources estimations, but is also regarded to be time-consuming and costly.

We have concluded that several popular current approaches to forecast production or estimate reserves and resources volumes are either too simple to handle the physical complexities of unconventional plays, or are time consuming and financially burdensome, and come with a steep learning curve. In addition, many methods do not readily quantify the level of uncertainty associated with a given forecast needed to comply with the low, best, and high recovery estimate categories (P10, P50, P90) in accordance with PRMS, or with SEC reporting standards.

1.5 Rate Transient Analysis

Rate transient analysis (RTA) is widely used as a diagnostic tool in industry to determine reservoir and completion parameters, however, RTA can also be used as a tool to estimate ultimate recovery in unconventional plays, as it does not require production or pressure history as a data input to generate a forecast. Unfortunately, methods to practically, probabilistically forecast production using RTA are not widely available: while a "best match" forecast generated with RTA can logically be viewed as a P50 (i.e., best or most likely) forecast, regulators and investors are far more interested in a range of recovery estimates, especially P90 (lower volume, high confidence) recovery estimates.

Existing RTA-based workflows available to generate a range of production forecasts (consistent with P10, P50, P90 PRMS and SEC guidelines) are sub-optimal: current industry software packages do not allow the user to easily forecast a probabilistic range of production forecasts automatically; rather, the individual forecasts which could comprise a probabilistic range must be generated one at a time.

While Monte Carlo Simulation (MCS) is often used to generate many results of an "experiment" at one time, often *thousands* of runs are required to yield a satisfactory range of results, many of which are redundant. Production forecasting with RTA also presents a challenge of "non-uniqueness," meaning several different combinations of input parameters can yield essentially the same production forecast, which could lead a user manually inputting many different input parameter combinations to arrive at a range of forecasts could be left with many redundant results, instead of an intended range of results. Except for very simple situations, MCS is not a practical alternative

for production forecasts with many uncertain reservoir and completion parameters, as in shales and other resource plays.

By incorporating DOE techniques, we can plan our "experiments"—the combinations of input parameters used to generate forecasts with RTA—more efficiently, to mitigate any potential cause for the generation of non-unique results. This not only reduces the number of runs to be performed, necessary to create a satisfactory range of forecasts, but also minimizes redundancy while maximizing our range of results.

1.6 Assumptions of this work

The following are assumptions we make in this work:

a. *Homogenous reservoir properties, and their implications*. Petrophyiscal properties such as permeability, porosity, formation height, etc., may not be homogenous throughout an unconventional play, however we assume fully homogenous formations in this work.

b. *Fracture stages and spacing*. We assume a single fracture per stage, and assume fracture spacing to be uniform for each of the simulated wells in this work, and assume that spacing equals lateral length divided by the number of fractures. This is also an assumption of the software model used in this work.

c. *Fully penetrating planar fractures*. Heterogeneous reservoir features may adversely impact the effectiveness of fracture stimulation treatments, ultimately resulting in fractures that only partially penetrate the height of the formation. While we assume that this may occur in some instances, we do not assess the effects of

anomalous, partially penetrating fractures in this work. The fracture half-lengths mentioned throughout this work are assumed to be uniform for each "well."

d. *Fracture conductivity levels.* We assume infinite fracture conductivity throughout the life of each well. This is also an assumption of the software model used in this work.

e. *Permeability.* We assume that permeability remains constant throughout the life of the well. This assumption is not required by the software model used in this work.

Reservoir Boundaries and Original Gas in Place (OGIP). The analytical model in the software which we used to validate our methods assumes a homogeneous, single-phase, rectangular reservoir, and a horizontal wellbore with equally spaced fractures along the length of the wellbore, and of equal specified half-length. This model, the "Horizontal Multifrac General Model", does not assume that reservoir dimensions are constrained by the dimensions of the completion; we do not specify any spacing between wells in this work. However, in some portions of this work, we assume OGIP is dependent upon SRV, and modeled by **Eq. 1:**

$$OGIP = \frac{2x_f L_{ex} h\varphi(1 - S_w)}{B_{gi}} \quad \text{.....} \quad (1)$$

B_{gi} is calculated using **Eq. 2** (Petrowiki, June 2018):

$$B_{gi} = 0.0282793 \frac{zT}{p} \quad \ldots\ldots\ldots\ldots\ldots\ldots\ldots\ldots\ldots\ldots\ldots\ldots\ldots\ldots\ldots\ldots\ldots\ldots\ldots\ldots\ldots\ldots \quad (2)$$

f. *Water Saturation (S_w), Oil saturation (S_o), and Gas saturation (S_g)*. For each simulated well, we assume constant S_w of 35%, S_o of 0%, and S_g of 65%.

g. *Single-phase flow.* We recognize this is a major limitation of RTA and have narrowed our focus to include only gas wells, and have assumed that these wells have no marginally significant oil, water, or other liquid production. This is also an assumption of the software used for validation purposes, in this work.

h. *Flow-back and/or invasion of fracture fluid.* During early time production, wells may produce "back" residual fracture fluid that has invaded the stimulated reservoir region, causing temporary, superficial, multi-phase flow (which cannot be accurately modeled with rate transient analysis). We will ignore any periods of early time water production in wells, always assuming single phase flow. However we will, if and when necessary, eliminate these anomalous monthly gas rates from any analysis of wells currently producing in the Barnett shale.

2. DATA COLLECTION AND METHODS

RTA is an attractive method to forecast production in that it considers the physical reservoir and completion characteristics of the well and of the reservoir, but does not require the time or financial commitment of a numerical simulator. However, RTA falls short as a production forecasting method in that it lacks the ability to *probabilistically* forecast production: the objective of this work is to develop a more practical approach to probabilistically forecast production in unconventional, undeveloped plays, using RTA. To develop and validate these approaches, it was first necessary to identify an area of interest, and gather sets of relevant input parameters required for RTA production forecasting relative to that area of interest.

2.1 Identified Area of Interest

The Barnett Shale is often regarded as the first unconventional play to be developed economically in the United States, the commercial development made possible by hydraulic fracturing and completion technologies. By 2005, the Barnett Shale produced nearly one trillion cubic feet of natural gas annually, the success of developing the play economically driving exploration and production companies to develop other previously untapped shale plays. We have chosen to focus on the Barnett Shale in the development of this work, in hopes that the literature and data of wells in this play is commensurate with its rich history.

Geographically limiting our study in this way enabled us to capture some variance of reservoir and completion parameters, while keeping the variance of each parameter

quite concentrated. Wells in Denton County are heavily concentrated toward the southwestern corner of the county, as shown in **Fig. 5**.

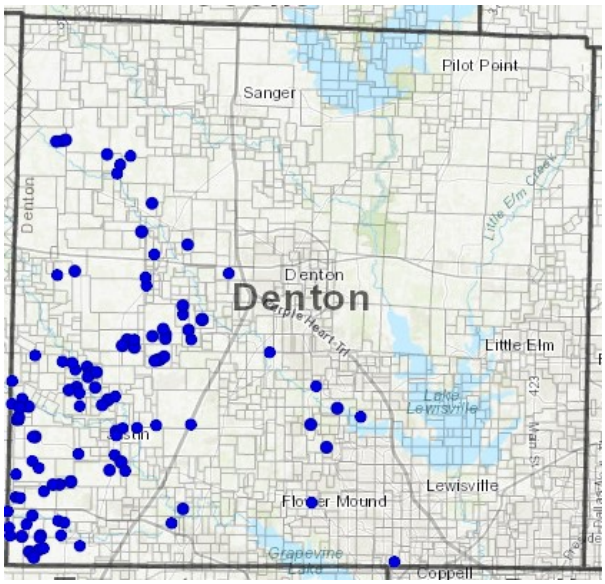

Fig. 5—Location of wells producing from the Barnett shale, Denton County, Texas. Adapted from DrillingInfo (2018)

Publicly available databases were used to extract information of 120 multi-fractured, horizontal gas wells (MFHWs) in the Barnett Shale, all in Denton County, Texas, and were studied to obtain necessary information about input parameters for this work. By narrowing our focus to wells in a limited geographic area, we are able to constrain the petrophysical heterogeneity among wells in the study, and make more reliable estimates of reservoir and completion properties for theoretical wells.

This group of 120 wells was chosen based on the amount of production history and amount of completion details publically available for each well: each of these 120 wells

had been producing for at least 60 months at the time of data collection, accompanied with a reported well depth, and reported lateral length. Probability distributions for each of the respective parameters were derived using this information.

2.2 Analytical Modeling in Commercial Software

The industry software program IHS Harmony (we refer to this as simply 'Harmony'), was used throughout this work to generate production forecasts using RTA. The input parameters required by Harmony to generate a single production forecast, as well as the parameters which are automatically calculated by the software, are listed in **Table 1.**

Table 1—Parameters required for production forecasting with RTA in Harmony

	Parameter	Description
Required input parameters	P_i	Initial pressure, psi
	P_{wf}	Flowing well pressure, psi
	x_f	Fracture half-length, ft.
	L_{ex}	Lateral Length, ft.
	FCD	Dimensionless fracture conductivity
	n_f	Number of fractures, #
	k	Permeability, nd/ md
	h	Formation height, ft.
	Φ	Porosity, %
	S_g	Gas saturation, %
	S_o	Oil saturation, %
	S_w	Water saturation, %
	T	Temperature, °R
Automatically calculated	c_f	Formation compressibility, psi^{-1}
	c_t	Total compressibility, psi^{-1}
	B_{gi}	Formation volume factor, (rcf/scf)
	X_e	Reservoir length, ft.
	Y_e	Reservoir width, ft.

While Harmony is robust and we assume the forecasts it generates with RTA are accurate, the program has limitations, primarily in that it does not allow for the

generation of more than one forecast at a time: in other words, a single set of parameters associated with a forecast must be input one at a time, to generate a single production forecast. This makes evaluating large numbers of wells extremely burdensome, especially when certain input parameters required to generate the forecasts are unknown, and when many different combinations of parameters can yield the same results with RTA. Additionally, there are currently no capabilities within Harmony to take into consideration any kind of economic parameters.

This software allows for the generation of probabilistic production forecasts with RTA, using Monte Carlo Simulation (MCS) techniques to randomly sample the probability distributions of each input parameter (these probability distributions are nominated by the user) and generate a range of forecasts, allowing the user to specify the number of random runs they would like to have performed. With MCS, however, thousands of forecasts need to be generated in order to arrive at a valid range, which is inefficient. Additionally, accurate probability distributions of reservoir and completion parameters are not often known, nor are they easily found; inputting probability distribution estimates that are not of great certainty yields inaccurate results. The inaccuracy of these results is only compounded when randomly sampling many uncertain probability distributions, with MCS.

In this work, we try to overcome these limitations, applying DOE techniques to reduce the number of runs required to compile a reliable probabilistic range of forecasts (based on quality of history match), and eliminate the necessity of having accurate probability distributions of each input parameter to generate a range of production

forecasts. DOE techniques are used to create a set of unique “treatment combinations”, which are then ranked based on best-fit history match of production data of a well. The treatment combinations which achieve a best-fit history match to production data are then used as input parameters to generate a production forecast, for that well. From this condensed range of best-fit forecasts, appropriate P10, P50, and P90 forecasts can be determined. We then assess how the forecasts generated this way, compare to forecasts generated using the same input parameters, with Harmony. We also assess how well the methods we present are able to accurately estimate unknown reservoir and completion parameters of a certain well.

The first step of our proposed workflow requires generating DOE treatment combinations, which serve as our history-match parameters, and as our parameters to forecast production. This requires, first, identifying the DOE technique that can configure the raw (reservoir and completion) information it is fed, in a way that best fits our needs. Prior to that, it requires we obtain the necessary and raw data we would like to be properly configured.

2.3 Data Collection

The required input parameters to forecast production using RTA in the IHS Harmony software, description of whether they will be varied or constant in our analysis, and how we obtained information about that parameter in our analysis, are listed in **Table 2**.

Table 2 —Input parameter descriptions

Parameter	Description	Constant/ Variable	Source (value if constant)
P_i	Initial pressure, psi	Constant/ Uncontrollable	Public well data
P_{wf}	Flowing well pressure, psi	Constant/ Uncontrollable	Assumed (500 psi)
x_f	Fracture half-length, ft.	Variable/ Controllable	Literature search
L_{ex}	Lateral Length, ft.	Constant/ Uncontrollable	Public well data
F_{CD}	Dimensionless fracture conductivity	Constant/ Uncontrollable	Assumed (Infinite)
n_f	Number of fractures, #	Constant/ Uncontrollable	Public well data
k	Permeability, nd/ md	Variable/ Controllable	Literature search
h	Formation height, ft.	Variable/ Controllable	Literature search
Φ	Porosity, %	Variable/ Controllable	Literature search
S_g	Gas saturation, %	Constant/ Uncontrollable	Assumed (65%)
S_o	Oil saturation, %	Constant/ Uncontrollable	Assumed (0%)
S_w	Water saturation, %	Constant/ Uncontrollable	Assumed (35%)
T	Temperature, °R	Variable/ Controllable	Public well data
c_f	Formation compressibility, psi^{-1}	Pressure-dependent	Calculated
c_t	Total compressibility, psi^{-1}	Pressure-dependent	Calculated
B_{gi}	Formation volume factor, (rcf/scf)	Pressure-dependent	Calculated

In the sections that follow, we discuss how probability distributions of each of the listed parameters in Table 2 were derived; "raw" information from those probability distributions were groomed by DOE techniques to compile the treatment combinations, which were used to history-match available production data, and used to generate production forecasts.

2.3.1 Initial Pressure, Lateral Lengths, Fracture Stages, and Temperature

Although not all parameters required as input to forecast production with RTA were not publically available, the RTA input parameters which *were* publically available (on a per-well basis) include total vertical depth, lateral length, fracture stages (we assume one fracture per stage), and initial bottom hole temperature. We estimate initial reservoir pressure using an assumed pressure gradient of .465 psi/ft.

Major input parameters necessary to generate production forecasts with RTA in Harmony which were not available in public well data include included fracture half length, dimensionless fracture conductivity, permeability, formation height, porosity, initial water saturation, initial gas saturation, initial oil saturation, fluid compressibility, and formation compressibility. Latitude and longitude data of the wells in our set, however, *were* publically available, and well locations were also used throughout the data collection process. We discuss their function in the following section.

2.3.2 Formation Height and Porosity

Supplementary to publicly available well data sets, a literature review of the Barnett shale was conducted in attempt to understand reasonable parameter ranges for the remaining unknown reservoir and completion parameters needed to forecast production using RTA. Fu et al. (2015) offer an in-depth look at the geological characterization of the Barnett Shale via geologic mapping of porosity, and net pay zone thickness maps. The locations of our wells were overlaid on to these geological maps to extract probability distribution estimates of formation height and porosity for our well set, as shown in **Fig. 6**.

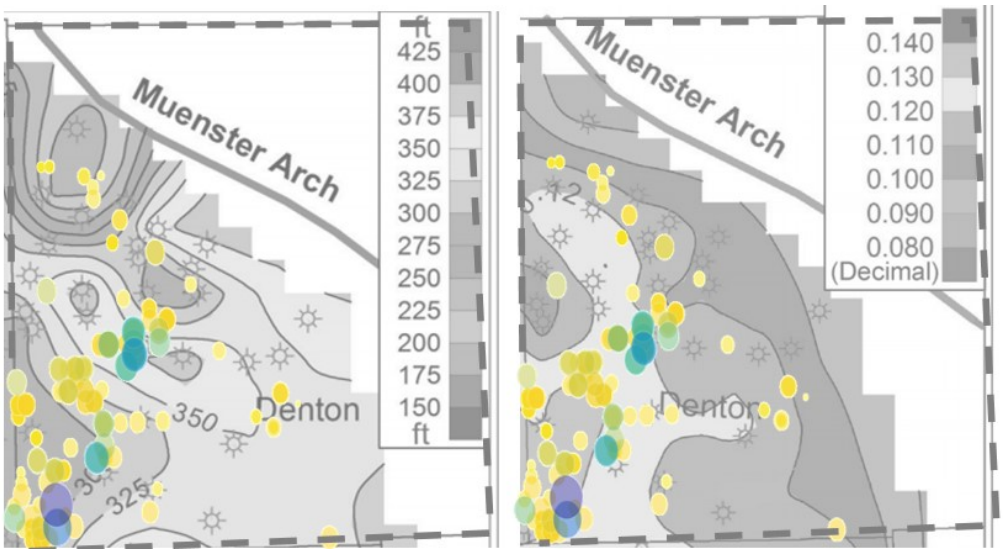

Fig. 6—Well locations overlaid on geologic maps of Barnett shale, Denton County, TX. Map reprinted from Fu et al (2015)

While Fu et al. explicitly report the mean, median, mode, standard deviation, and ranges for porosity for the entire play, it is clear from the maps that the probability distributions of porosity for wells in Denton County will likely be much different than the porosity levels of the entire play. The best-fit probability distribution of porosity is shown in **Fig. 7**; for our study, we assume a range of porosity between 5.5%-7%.

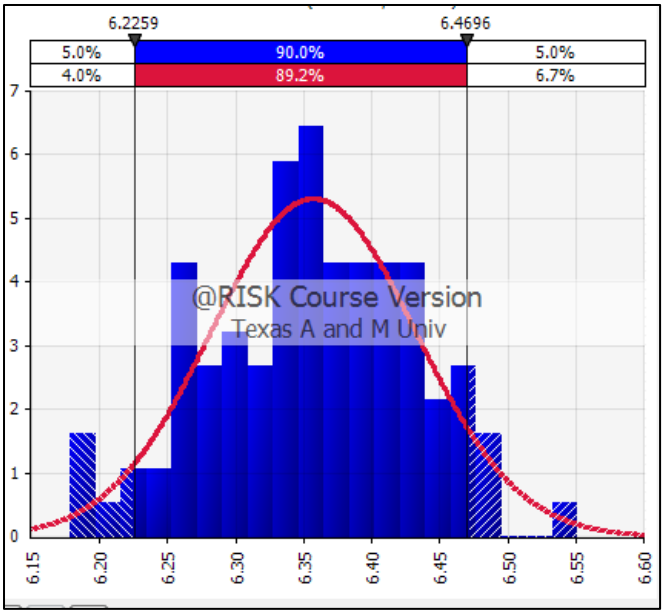

Fig. 7—Estimated probability distribution: porosity

The same procedure used to develop a probability distribution for porosity was performed to extract information about net pay thickness. The best-fit probability distribution of net pay thickness is shown in **Fig. 8.**

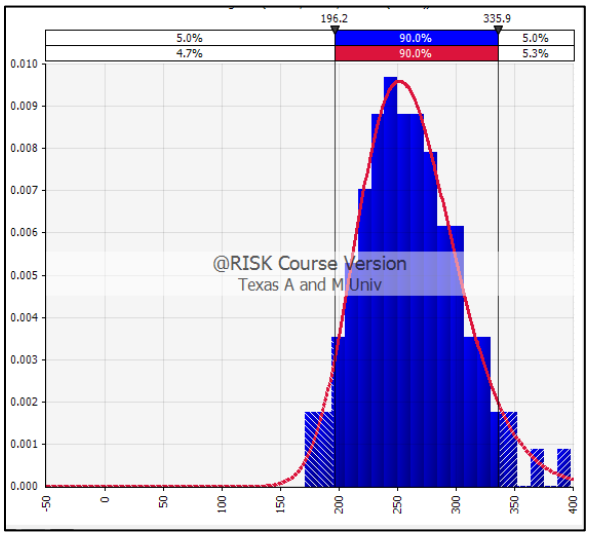

Fig. 8— Estimated probability distribution: net pay thickness

By overlaying our well locations onto the geologic maps of Fu et al., we were able to derive probability distributions of net pay thickness to be used in our analysis. For our study, we assume a range of porosity between 175 feet and 375 feet.

2.3.3 Fracture Half-Length

Fracture half-length is a parameter that is seldom known (often determined from diagnostic plots), and one that greatly impacts production levels. Cherian et al. (2009) presented a probabilistic distribution of fracture half-lengths for MFHWs, reporting a lognormal distribution with a mean value of 285 ft., P90 value of 123 feet, and a P10 value of 504 feet; however, the focus of their work in the Piceance Basin (this distribution is shown in **Fig. 54**). Yu et al. (2013) study the optimization of MFHWs in the Barnett shale, having run experiments with varying fracture half-lengths uniformly distributed with a range from 200 feet to 400 feet.

The range of fracture half-length values used in this work is conservative in that we honor values reported by Yu et al., but extend the minimum end of the range as low as 100 feet, consistent with the minimum values of fracture half-length reported by Cherian et al. Because most reservoir and completion parameters are distributed lognormally, we combine the two aforementioned distributions of fracture half-length and assume our fracture half-lengths are characterized by a probability distribution with a P90 value of 100 feet, and a max value of 400 feet, which translates best into a lognormal distribution with a mean value of 201 feet, a P90 value of 100 feet, and a P10 value of 339 feet. This best fit probability distribution is shown in **Fig. 9**.

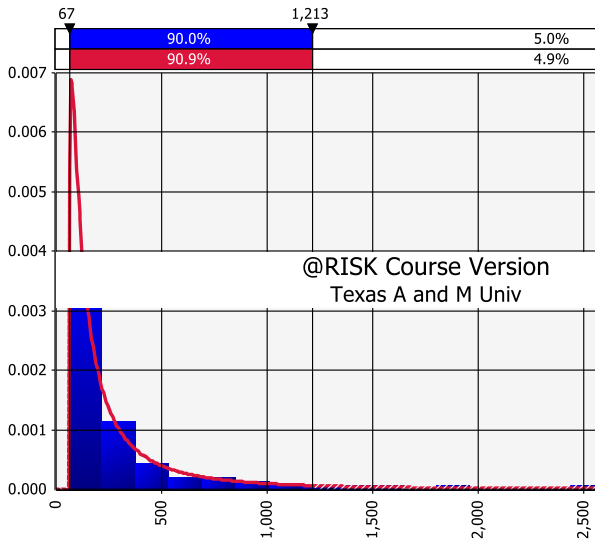

Fig. 9— Estimated probability distribution: fracture half-length

2.3.4 Permeability

The ultra-low permeability values of unconventional plays are the primary obstacle which must be overcome to produce economically from these plays. Permeability is a reservoir parameter which greatly affects production levels, and one that is highly variable within unconventional plays: because permeability data is not made publicly available on a per-well basis, the range of permeability values used in this work was compiled from a variety of literature sources, from which many different ranges of permeability values from the Barnett shale were reported.

The range of permeability established for this work is an amalgamation of the Barnett permeability ranges suggested in literature: DrillingInfo suggests an average permeability of the Barnett Shale of 250 nd. Ezisi et al. (2012) suggest a range between 70 nd to 500 nd. Anderson et al. (2012) utilize a SRV permeability between 100 nd and 5000 nd in their work. For this work, we consider a range based off a lognormal

distribution for permeability, with a P90 of 80 nd, and a P10 value of 750 nd. The mean of the permeability probability distribution for this work is 168 nd. This distribution is shown in **Fig. 10**.

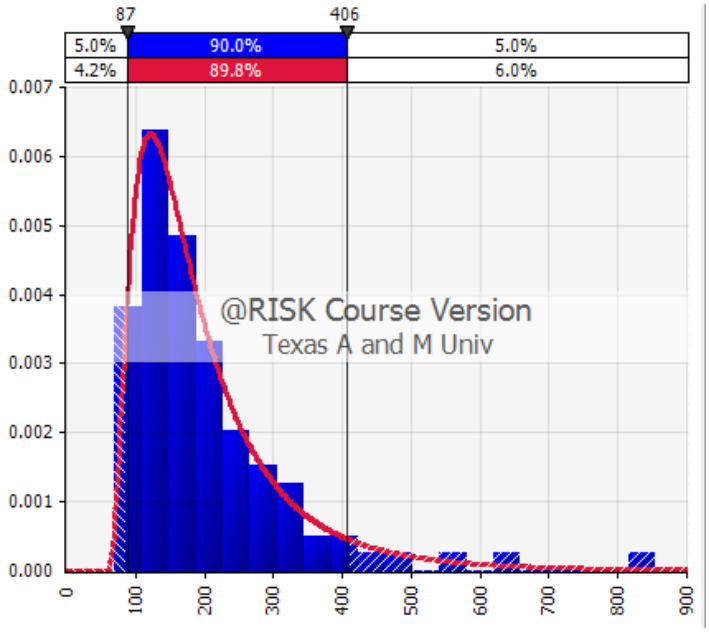

Fig. 10— Estimated probability distribution: permeability

2.4 Experimental Design

After making estimates of the parameters of the Barnett shale which would eventually be used to forecast production with RTA techniques (and validated in Harmony), we then investigated Experimental Design techniques and how they could be implemented to streamline the process of probabilistically forecasting production using RTA.

Experimental Design (ED), or the *Design of Experiments (DOE)*, is a family of techniques that can aid in the optimization of performing experiments. Choosing the most appropriate DOE technique for a given experimentation process depends on the format and the objective of the experiment itself, and on the intent of the project owners. An "experiment" can be defined broadly as a process of data collection with the intent of gathering enough information about the effects of changing conditions, variables, or "factors" on the outcome, result, or "response", to either make conclusions, or make predictions about, future responses. "Control variables" are those variables in an experiment that are held constant, usually to put more focus on the effects of the independent, "uncontrollable variables." DOE can be regarded as the planning and organization of an experiment before it takes place, to reduce redundancy, ensure the appropriate data is being used to achieve such objectives, and to achieve results and conclusions of experiments in a more efficient manner.

With this background in mind, we can consider production forecasting and the process of estimating ultimate recovery for a given area, using RTA, as an experiment: engineers must perform many different "runs"—using many different combinations of varying parameters (many of which are seldom known with certainty) —to eventually achieve many individual "results", a satisfactory probabilistic range of recovery estimates or production forecasts. Monte Carlo Simulation (MCS) is often used as a tool to generate many results, to form a "complete" range of possible scenarios. As it applies to history-matching and production forecasting with RTA, MCS can require thousands of runs be executed to return a full distribution, only three (!) of which are required for PRMS and SEC reserves and resources reporting purposes.

When production forecasting with RTA, there is an inherent challenge of non-uniqueness: more than one combination of input parameters into this analytical model can yield similar results: when MCS is used in the experimentation process of production forecasting, many of the runs generated are redundant, due to this challenge of non-uniqueness. Especially if an engineer is manually inputting runs—different combinations of parameters—in effort to achieve a satisfactory history match with any pre-existing production history, it is valuable to know which combinations will generate negligible results. When some production history of a well is known, the treatment combinations generated with DOE techniques can be used to history match for unknown reservoir and completion parameters, and subsequently be used to generate production forecasts.

DOE aids us in identifying the combinations of input parameters ("treatment combinations") that will allow us to survey the entire "experimental region" more efficiently, by determining on a statistical basis, which unique combinations of input parameters will yield the most impactful results, maximizing the experimental region in a minimal number of runs, reducing redundancy in the results in our experiments, saving us time and resources. We describe DOE, graphically, in **Fig. 11**.

Representing experimental design visually: (A) an experiment (in-progress), carried out without DOE techniques, is performed in a locally and inefficient way. (B) A complete experiment carried out without DOE techniques allows us to see "full coverage" of the experimental region, however there is some risk that some results may be redundant, or negligible. (C) An experiment run using DOE techniques creates locally unbiased runs, which allows us to see the same maximized coverage of the

experimental region in (B), but in many less runs, as the results of *every* experiment are not surveyed.

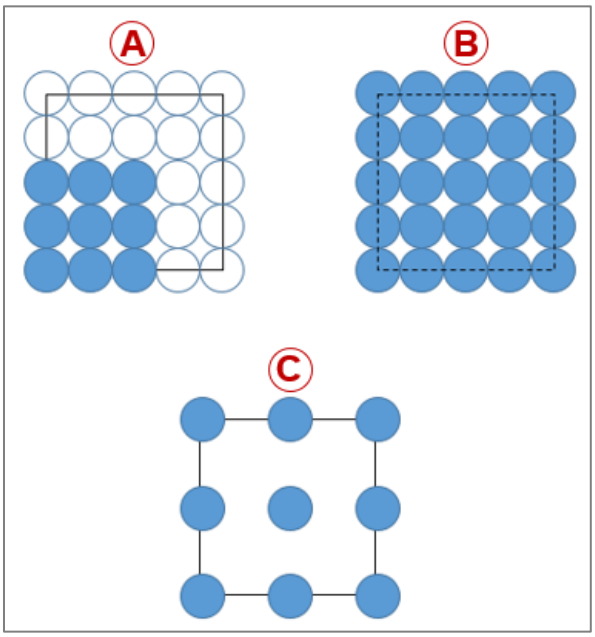

Fig. 11—Experimental design: Efficiently maximizing the design space

In DOE, the experimental variables are referred to as *factors*, the values of which those factors can be varied are referred to as *levels.* We explain this, and other DOE terminology, in **Fig. 12**: the experiment described in Fig. 11 is a 3-factor, 2-level experiment (each factor in each trial is either a "+" or a "-").

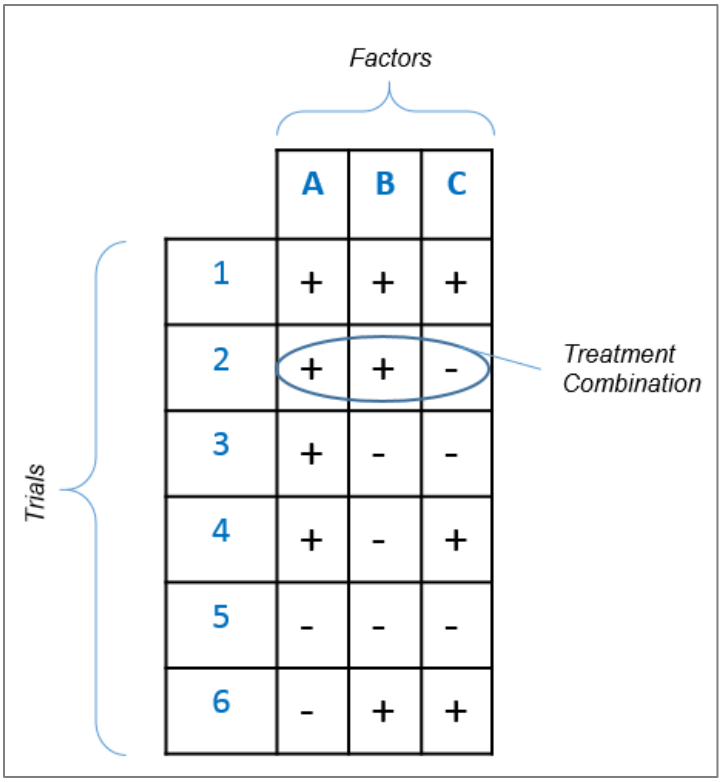

Fig. 12—Graphical explanation of DOE terminology

Many classical DOE techniques only consider two "factor levels", or, binary variation of any "controllable" parameter within the experiment. Because forecasting production with RTA probabilistically is an "experiment" that requires many different "factors" (input parameters) and "factor levels" (range of parameter values) to generate each forecast in a probabilistic range, classical DOE techniques did not apply, which quickly narrowed the pool of possible DOE techniques that could be integrated into this work: to investigate production forecasting and EUR estimation using RTA thoroughly, more than two levels for each factor need to be considered.

The DOE approach we identified to be the most consistent with the objectives of this work is "D-Optimal Design." D-Optimal designs use raw factor, and raw factor level data input by the user, to return a set of optimal "treatment combinations" to be run in the experimental process. These treatment combinations are the unique combinations of factors which are said to "maximize the design space." D-Optimal designs allow the user to nominate more than two levels of each factor, and also allow the user to nominate the number of trials (treatment combinations) to be conducted in the experiment, to construct the optimal set of treatment combinations based on the maximum D-Optimal criterion (which is the maximum of |X'X|, the determinant of the information matrix X'X) (www.itl.nist.gov, March 2018). The algorithm used to determine this optimal set of treatment combinations first analyzes all possible combinations of input parameters, and through a step-and-exchange process, identifies the combinations which to include in the final "design" (www.itl.nist.gov, March 2018).

With D-Optimal design, the user has some freedom to specify the number of "trials" to be returned in the final design. However, the minimum number of trials that must be included for the design to be considered "efficient" does depend somewhat on the number of factors and factor levels the user wishes to include in an experiment: the quality of a set of trials created with D-Optimal designs lies in its D-efficiency value. D-Optimal design techniques are deemed "optimal" if the D-efficiency metric (included in the output of the DOE software) is greater than or equal to 0.7. For this work, the number of trials nominated and utilized for our experiments ranged from 36 trials (the maximum for a two-factor, six-level experiment, when history matching

production to determine reservoir and completion parameters, when many parameters are already known) up to 1,000 trials (for a 4-factor, 6-level experiment, when history matching and forecasting production for wells, when less parameters are "known"). In any case, the trials identified to be among the "top" 20 to 50 (based on quality of history-match) were used to generate production forecasts.

In this work, we will feed the DOE software six to seven raw levels—discrete values—of each "controllable" factor (reservoir and completion parameters), to configure treatment combinations which will be used in the history matching and production forecasting processes in this work. Although we realize the controllable factors in our analysis are not always necessarily *controllable*, we have chosen to vary them in our analysis as they are all parameters with high influence on production levels and ultimate recovery, and known with little certainty.

2.5 Workflow: using diagnostic plots to history match and forecast production

We discussed that although the experiments we designed consisted of up to 1,000 trials (or treatment combinations), only the best-fitting 20 to 50 treatment combinations were used to generate production forecasts for each well. We discuss the process used to identify these top-ranked treatment combinations in this section, in addition to discussing how production forecasts were then generated from those top-ranking combinations.

Wattenbarger (1998) originally proposed **Eq. 3(3**, to determine contacted surface area (A) and permeability (k) for shale gas wells producing in transient linear flow.

$$A\sqrt{k} = \frac{1262}{m_{cp}\sqrt{\varphi\mu c_t}} \times \frac{T}{m(p_i) - m(p_{wf})} \quad \ldots\ldots\ldots\ldots\ldots\ldots\ldots\ldots\ldots\ldots\ldots\ldots \quad (3)$$

Where

$$A = 4x_f h \quad \ldots\ldots\ldots\ldots\ldots\ldots\ldots\ldots\ldots\ldots\ldots\ldots\ldots\ldots\ldots\ldots\ldots\ldots\ldots\ldots \quad (4)$$

Eq. 3 assumes that all other parameters—reservoir temperature (T), porosity (φ), viscosity (μ), and total compressibility (c_t)—in the reservoir are known, and uses the parameter m_{cp}, which is the slope of the gas normalized pressure vs. $\sqrt{t}$ diagnostic plot. An example of that plot is shown in **Fig. 13.**

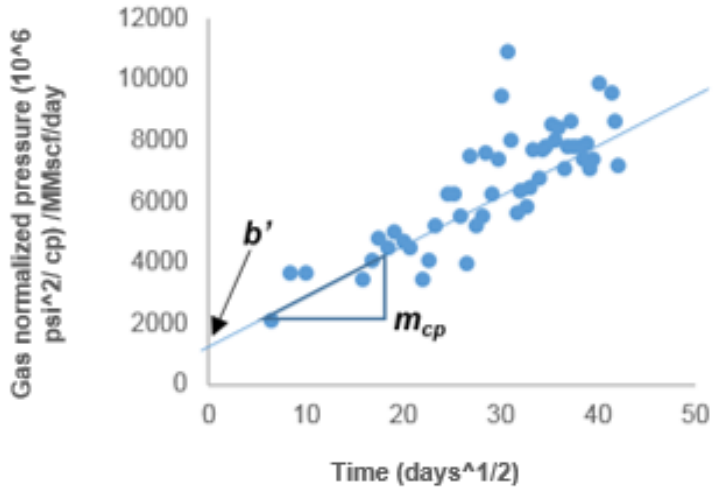

Fig. 13—Gas normalized pressure vs. $\sqrt{t}$ plot

The trend line shown in the gas normalized pressure plot (Fig. 13), is an expression for gas normalized pressure. This expression can be written in terms of m_{cp} and b', shown in **Eq. 5** (Fekete, 2018).

$$\frac{m(p_i) - m(p_{wf})}{q} = m_{cp}\sqrt{t} + b' \qquad \text{..... (5)}$$

Where $m(p_i)$ and $m(p_{wf})$ are pseudo-pressures of initial reservoir pressure (p_i) and well flowing pressure (p_{wf}), respectfully. The parameter b' in Eq. 5 is considered to be a metric of completion effectiveness, indicative of skin and finite fracture conductivity.

Rearranging Eq. 5, m_{cp} can be expressed in terms of rate (q) and time (t), in **Eq. 6:**

$$m_{cp} = \frac{\frac{m(p_i) - m(p_{wf})}{q}}{\sqrt{t}} \quad \ldots\ldots\ldots\ldots\ldots\ldots\ldots\ldots\ldots\ldots\ldots\ldots\ldots\ldots\ldots\ldots \quad (6)$$

To generate production forecasts with our proposed workflow first requires the well to be history matched. A "target" m_{cp} value (we will refer to the target m_{cp} as $m_{cp\underline{T}}$) will be calculated using Eq. 6 for each well to be forecasted, based on the well's available production history. This target $m_{cp\underline{T}}$ value serves as our history matching parameter.

We then rearrange Eq. 3 in terms of m_{cp} (not $m_{cp\underline{T}}$), expand the A term, and rearrange the equation so the known parameters of the well to be forecasted lie in the first term, while unknown parameters lie in the second term in **Eq. 7:**

$$m_{cp} = \frac{1262 \times T}{4\sqrt{\mu c_t} \times [m(p_i) - m(p_{wf})]} \times \frac{1}{x_f h \sqrt{k\varphi}} \quad \ldots\ldots\ldots\ldots\ldots\ldots\ldots\ldots\ldots\ldots\ldots\ldots \quad (7)$$

For each trial (or treatment combination) generated using DOE techniques (in some cases, up to 1,000 trials, as we discussed in previous sections), an m_{cp} value was calculated using Eq. 7, having input each trial's unique combination of parameters. In an appropriately formatted Excel spreadsheet, this requires essentially no computational time.

We assume that during transient linear flow, all variables (with the exception of time) remain constant. Viscosity (μ), and total compressibility (c_t), are approximated for each trial based on p_i, using a helpful tool created and made publically available by

the University of Louisiana at Lafayette (University of Louisiana at Lafayette, 2018). From this tool, c_g is approximated. We then assume that c_t can be approximated by **Eq. 8** (assuming S_g = 65% for each trial).

$$c_t = c_g \times S_g \quad \ldots\ldots\ldots\ldots\ldots\ldots\ldots\ldots\ldots\ldots\ldots\ldots\ldots\ldots\ldots\ldots\ldots\ldots \quad (8)$$

The treatment combinations were then ranked, based on how closely their calculated m_{cp} values matched the $m_{cp\underline{T}}$ value of the well to be forecasted (based on lowest sum of squared error, or SSE).

So, although not all generated treatment combinations were used to generate production forecasts, all treatment combinations were contenders during the history matching process. As discussed, only the best 20-50 top-ranking trials (again, based on calculated m_{cp} deviation from $m_{cp\underline{T}}$ value of well to be forecasted) were used to generate production forecasts; more specifically, the m_{cp} value of each trial identified as a "top" match was used to generate a production forecast, using a rearrangement of Eq. 6, shown in **Eq. 9:**

$$q = \frac{m(p_i) - m(p_{wf})}{m_{cp}\sqrt{t} + b'} \quad \ldots\ldots\ldots\ldots\ldots\ldots\ldots\ldots\ldots\ldots\ldots\ldots\ldots\ldots\ldots\ldots\ldots\ldots \quad (9)$$

Using Eq. 6, Eq. 7, and Eq. 9 allows us to perform history matches, and to extrapolate production forecasts, for MFHWs with short production histories and limited reservoir and completion information. This workflow is described in **Fig. 14.**

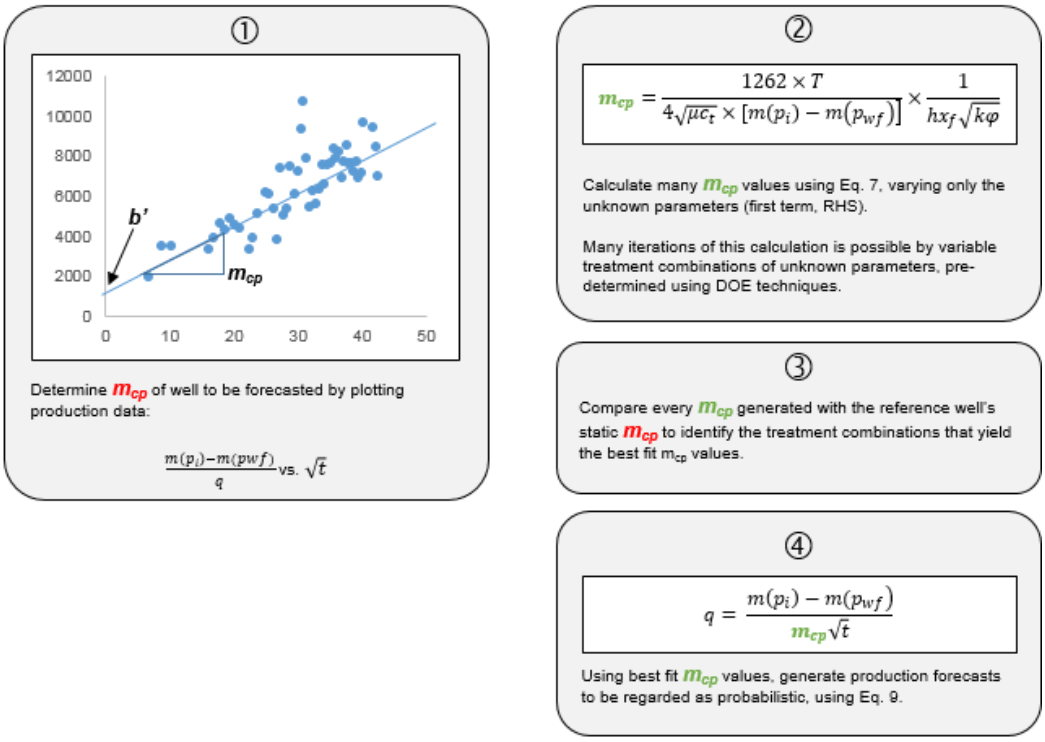

Fig. 14—History Match Workflow

Explaining the workflow shown in Fig. 14 further: Eq. 7 is used to calculate many possible values of m_{cp}, using treatment combinations devised using DOE techniques, (which we discuss in the following section). Incorporating DOE techniques allows us to estimate unknown reservoir and completion parameters, based on which treatment combinations—when used in coordination with the known parameters of a given well—yield an m_{cp} value closest to the well's true m_{cpT} value.

Independent methods are needed to forecast production in transient linear flow (early time), and to forecast production in boundary-dominated flow (BDF) (late time). The time at which the method used to forecast changes is the time at which pressure changes in the reservoir due to production have reached the outermost boundary of the reservoir (Wattenbarger et al., 1998). Estimating this transition time, the time to end of linear flow, t_{elf}, is critical in properly estimating production rates.

The time to end of transient linear flow (t_{elf}) is estimated using **Eq. 10** (Fekete, 2018):

$$t_{elf} = \left(\frac{d_i \sqrt{\varphi \mu c_t}}{2 \times .159 \sqrt{k}} \right)^2 \quad \ldots\ldots\ldots\ldots\ldots\ldots\ldots\ldots\ldots\ldots\ldots\ldots\ldots\ldots\ldots\ldots \quad (10)$$

Where μ and c_t are estimated for each run using the tool available through the University of Louisiana at Lafayette (and dependent on a "random" p_i value determined by DOE techniques). In Eq. 10, k is also determined randomly by DOE techniques. The value of φ is kept constant at 6.0% throughout this work.

We calculate d_i to be the half-distance between two fractures, using **Eq. 11:**

$$d_i = \frac{L}{2 * n_f} \quad \ldots\ldots\ldots\ldots\ldots\ldots\ldots\ldots\ldots\ldots\ldots\ldots\ldots\ldots\ldots\ldots \quad (11)$$

Where L and n_f are known parameters of the well to be forecasted.

Eq. 10 could also be expressed in terms of x_f, as we present in **Eq. 12** (Fekete, 2018):

$$t_{elf} = \left(\frac{A\sqrt{\varphi \mu c_t}}{4 \times .159\, x_f \sqrt{k}} \right)^2 \quad \ldots\ldots\ldots\ldots\ldots\ldots\ldots\ldots\ldots\ldots\ldots\ldots\ldots\ldots\ldots\ldots \quad (12)$$

Production during boundary-dominated flow was then estimated using Arps' hyperbolic decline model, shown in **Eq. 13.**

$$q = \frac{q_i}{(1 + bD_i t)^{\frac{1}{b}}} \quad \ldots\ldots\ldots\ldots\ldots\ldots\ldots\ldots\ldots\ldots\ldots\ldots\ldots\ldots\ldots\ldots\ldots\ldots\ldots\ldots \quad (13)$$

The *b*- parameter used to forecast production in this work is kept constant at b = 0.4; Fetkovich et al. (1996) as well as Lee and Sidle (2010) suggest using this value for *b* when using Arps' to forecast production in gas wells, when p_{wf} is approximately equal to 10% of p_i. This condition is consistent with the assumptions of this work.

When forecasting production with Eq. (13), we assume q_i to be the last monthly production rate of the well while in a transient flow period.

The D_i – parameter used for this work is estimated for each individual forecast, by rearranging Eq. (13), as shown in **Eq. 14:**

$$D_i = \frac{(\frac{q_0}{q_t})^{.4} - 1}{.4 t_{elf}} \quad \ldots\ldots\ldots\ldots\ldots\ldots\ldots\ldots\ldots\ldots\ldots\ldots\ldots\ldots\ldots\ldots\ldots\ldots\ldots\ldots \quad (14)$$

Where q_0 is the first appropriate and representative forecasted production rate during the transient flow period, q_t is the last forecasted production rate during the transient flow period (the same as q_i), t is replaced by t_{elf}, and where we have replaced the b -parameter in Eq. 13 with .4.

2.6 Incorporating DOE Techniques into History Matching and Production Forecasting with RTA

Because of the challenge of non-uniqueness presented when history-matching and generating a production forecast with RTA, it is difficult to predict which combinations of parameters will yield a unique forecast: DOE pre-determines the combinations of input parameters that we will use to history match and forecast production, reducing the work required to generate these combinations on our own, while reducing the number of runs required to form a "complete" experiment, by mitigating redundant results. We describe graphically, how DOE treatment combinations are incorporated into the history matching process, in **Fig. 15.**

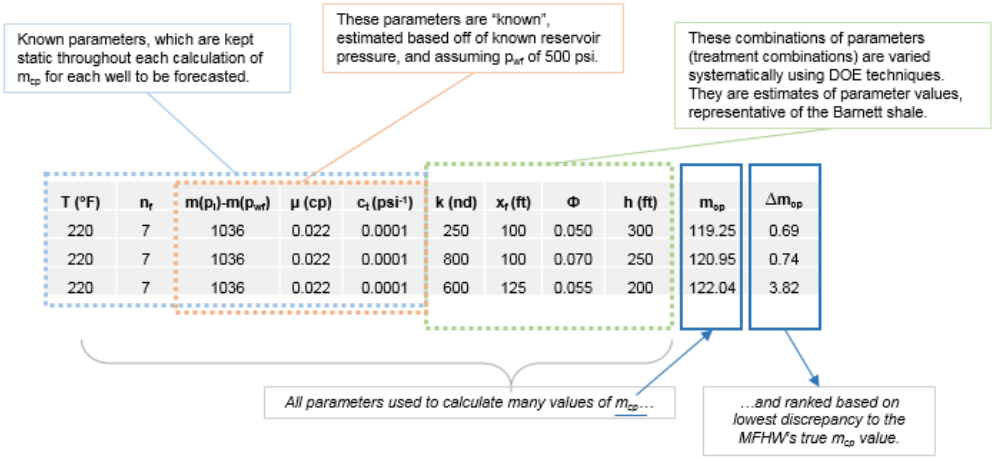

T (°F)	n_f	$m(p_i)-m(p_{wf})$	μ (cp)	c_t (psi^{-1})	k (nd)	x_f (ft)	Φ	h (ft)	m_{cp}	Δm_{cp}
220	7	1036	0.022	0.0001	250	100	0.050	300	119.25	0.69
220	7	1036	0.022	0.0001	800	100	0.070	250	120.95	0.74
220	7	1036	0.022	0.0001	600	125	0.055	200	122.04	3.82

Fig. 15—Incorporating DOE into the history matching process

Preparing a worksheet to perform the workflow we describe above, in a program such as MS Excel, allows us to calculate thousands of potential m_{cp} values (and identify previously unknown reservoir and completion parameters of a well) in a matter of seconds. Once the best-matched m_{cp} values for a given well are established, a range of production forecasts—from which forecasts that can be regarded as probabilistic P10, P50, P90 forecasts can be extracted—can be generated just as quickly.

2.7 Summary

In this chapter, we have identified the Barnett shale as our area of interest, and explained the literature search that was performed to develop probability distributions of reservoir and completion parameters. We explained that discrete values from these probability distributions were fed into a DOE software, where D-Optimal design

algorithms were employed to develop efficient sets of treatment combinations, to be used in history-matching existing production data of wells, and subsequently, generating production forecasts.

We suggest using D-Optimal design techniques as a DOE method as we do in this work, to simplify the process of probabilistically forecasting production with RTA: we conclude that D-Optimal designs are helpful as when "randomly" creating experimental runs, but also helpful when the effects of certain input parameters vary discretely and definitively (such as completion parameters, when decimal change to parameters such as lateral lengths and number of fractures tend to be negligible).

3. RESULTS

In this chapter, we forecast production for Barnett Shale MFHWs using the simplified approach which we have presented. We then apply the workflow throughout the history-matching process, but generate production forecasts using a software which allows for forecasting production with RTA, and compare our results.

3.1 Application of workflow to history match and forecast production for Barnett shale MFHWs

The workflow described in Section 2.5 was used to history match, and generate a range of production forecasts, for several MFHWs currently producing in the Barnett shale. The generated forecasts compared with the true production rates of several wells are reviewed in Section 3.1.5, however we first highlight two particular wells ("Well D" and "Well K" more in depth in Sections 3.1.1 through 3.1.4.

3.1.1 Forecasting production for Well D, 12-month history match and 60-month history match

The first step of our production forecasting workflow involves determining the slope ("target" m_{cp}, or $m_{cp\underline{T}}$), and intercept (b') of the gas normalized pressure vs. $\sqrt{t}$ plot, for the well to be forecasted. This may be done with any amount of production data available; it is critical when working with this diagnostic plot that the analyst remove any anomalous production rates from the plot to arrive at an accurate representative $m_{cp\underline{T}}$ value.

We present an example of this initial diagnostic plot in **Fig. 16**, which includes both 12 months and 60 months of production data to showcase that it may be possible that more than one trend line (and subsequently, more than one m_{cp} and b' values) could be detected, depending on how much production data is being analyzed, or vary depending on the time increment analyzed.

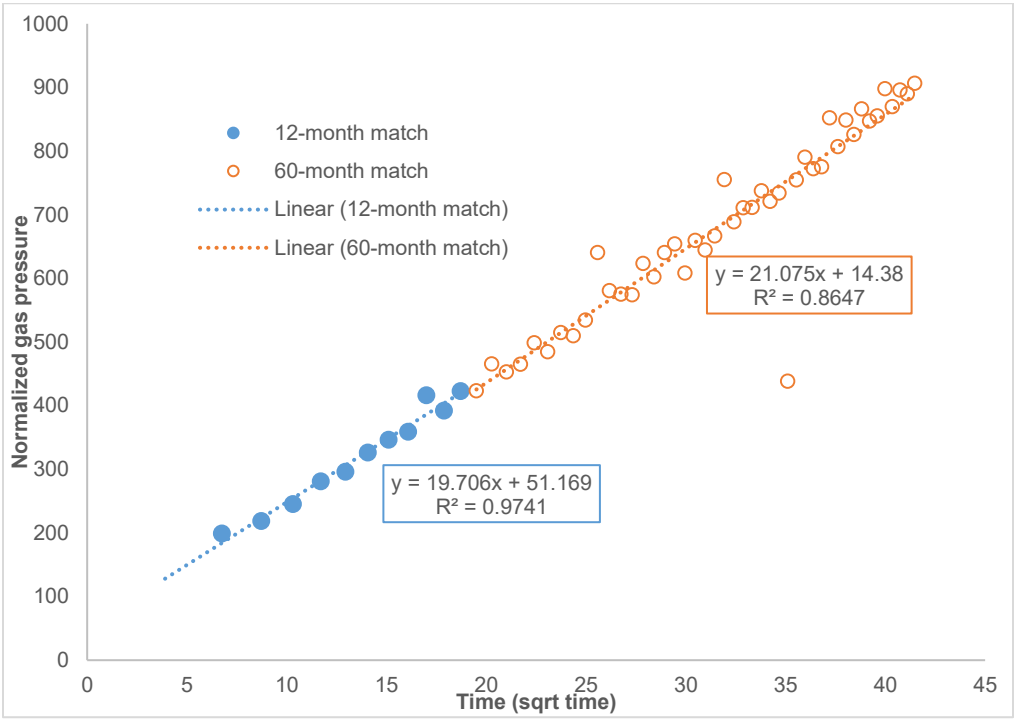

Fig. 16— Assessing m_{cp}: Well D

Fig. 16 showcases the normalized pressure vs. $\sqrt{t}$ plot for a MFHW ("Well D") currently producing gas from the Barnett shale. We can see that for Well D, there is a clear primary trend of the data regardless of the amount of production data being analyzed, and that neither m_{cpT} nor b' changes drastically from an analysis of 12 months, to 60 months, of production data.

For this portion of work, we systematically vary four parameters, fracture half-length (x_f), porosity (φ), formation height (h), and permeability (k), using DOE techniques for the history matching portion of our workflow. Six levels of each factor (x_f, φ, h, and k) were input into a DOE software to generate 1,000 treatment combinations. These factor levels are shown in Table 3, and drawn from the probability distributions of parameters shown in Section 2.3. Using the 1,000 treatment combinations, and with known parameters of Well D (number of fractures, n_f, initial pressure, p_i), assumed parameters of Well D (flowing well pressure, p_{wf},) and estimated parameters of Well D (pseudo-pressures, total compressibility, c_t, and viscosity, μ) 1,000 m_{cp} values were calculated for Well D.

Table 3—Factors and Factor levels input into DOE software, estimated reservoir and completion parameters, Barnett Shale

Parameter	Description	Units	Factor levels input into DOE software					
x_f	Fracture half-length	ft.	100	125	200	250	300	350
h	Formation height	ft.	175	250	300	325	350	375
k (outer)	Permeability	nd	80	100	250	400	600	800
phi	Porosity	%	0.04	0.05	0.055	0.06	0.065	0.07

1,000 treatment combinations were generated using the factor levels listed in Table 3 in a DOE software. Generating these 1,000 combinations of parameters, using DOE techniques, requires less than eight seconds. These combinations, in addition to the known parameters of Well D (number of fractures, n_f, initial pressure, p_i), assumed parameters of Well D (flowing well pressure, p_{wf},) and estimated parameters of Well D

(pseudo-pressures, total compressibility, c_t, and viscosity, μ) were used to calculate a m_{cp} value for each of the 1,000 aforementioned treatment combinations.

These treatment combinations were then ranked based on how closely their calculated m_{cp} values matched the target $m_{cp\underline{T}}$ value of Well D (determined from the diagnostic plot shown in Fig. 16, using the 12-month production data and trend line). The m_{cp} values which most closely matched the $m_{cp\underline{T}}$ value of Well D were then used to generate production forecasts during the transient flow period. As mentioned in Chapter 2, an independent method is needed to forecast production during BDF: for every best-matched treatment combination, a unique t_{elf} and D_i will be estimated, and a b-parameter of .4 will be used to estimate production in BDF using Arps' decline relations.

In **Fig. 17**, we show the 40 best-matched forecasts, matched on 12-months of production history, and compare the forecasts to the 60 months of true production data for Well D.

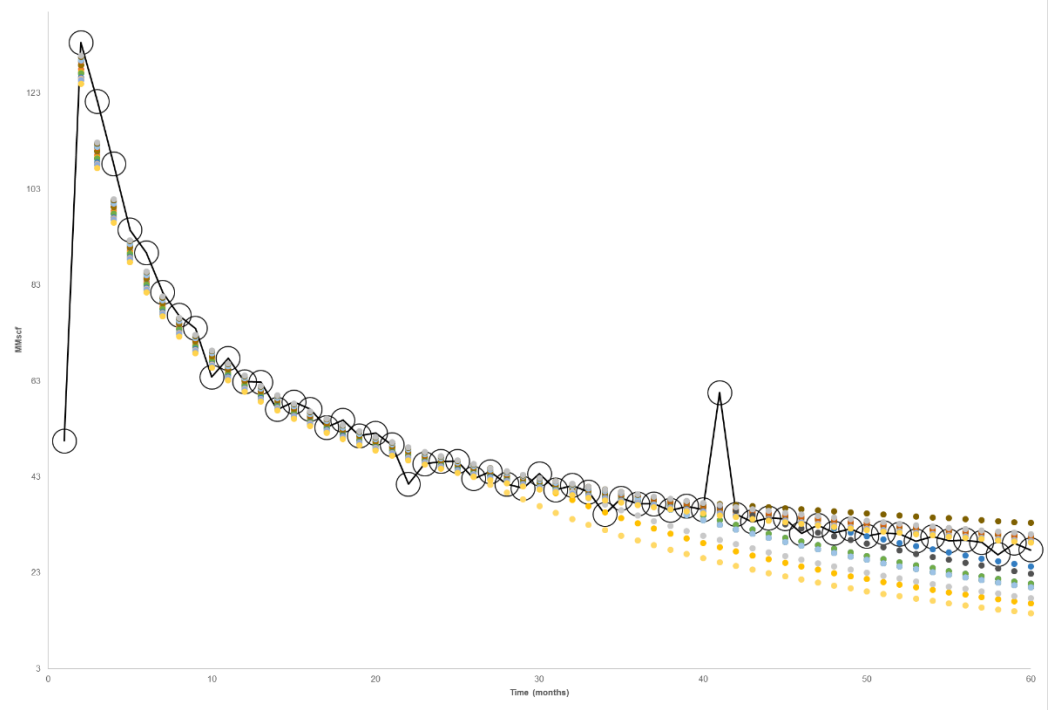

Fig. 17—Well D, 12-month history match and forecasts, months 0-60

In **Fig. 18** and **Fig. 19**, we parse this forecast into smaller time increments, to analyze the quality of the forecasts generated on the basis of a 12-month history match, more closely.

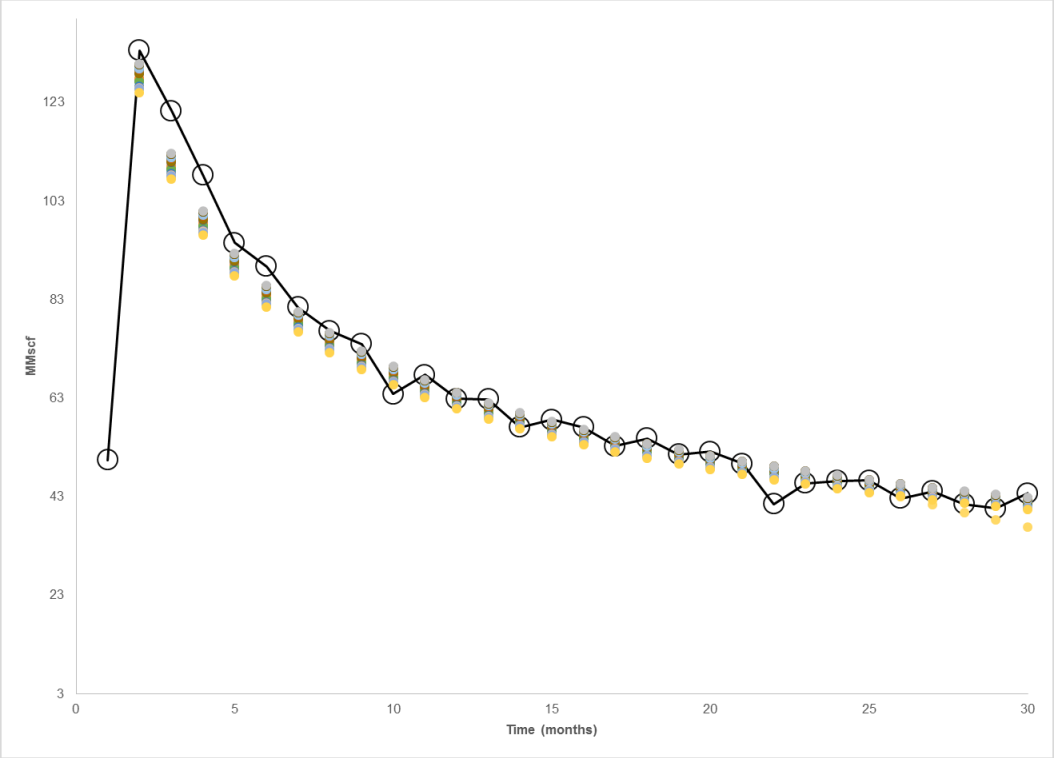

Fig. 18—Well D, 12-month history match and forecasts, months 0-30

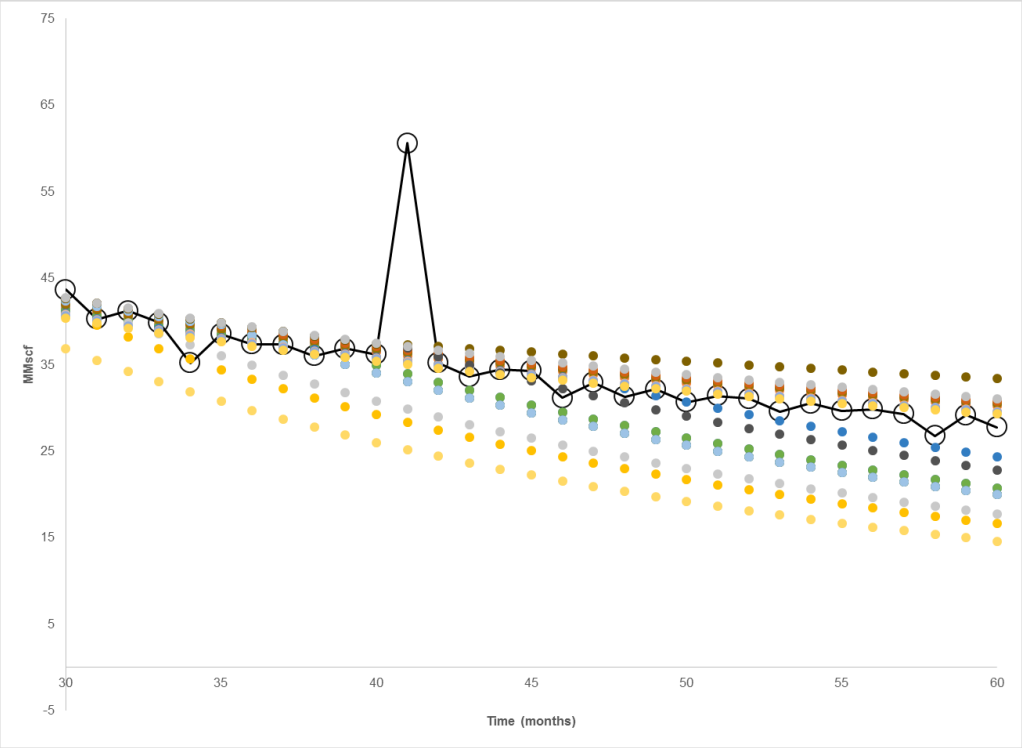

Fig. 19—Well D, 12-month history match and forecasts, months 30-60

The forecasts shown in Fig. 17 through Fig. 19 match the true production data of Well D satisfactorily for months 0-60, when history-matched with only 12 months of production data. Because when history-matching and forecasting on only 12 months of production data, we have no inclination of when exactly the transition from transient flow to BDF will occur, it can be seen from Fig. 17 through Fig. 19 that some best-fit forecasts (best-fit to 12 months of production data) towards the end of the 60 months forecasting duration may not capture this transition time properly. To analyze to what degree the forecasts estimated this time properly, we show a log-log plot of rate vs. MBT for Well D, in **Fig. 20**.

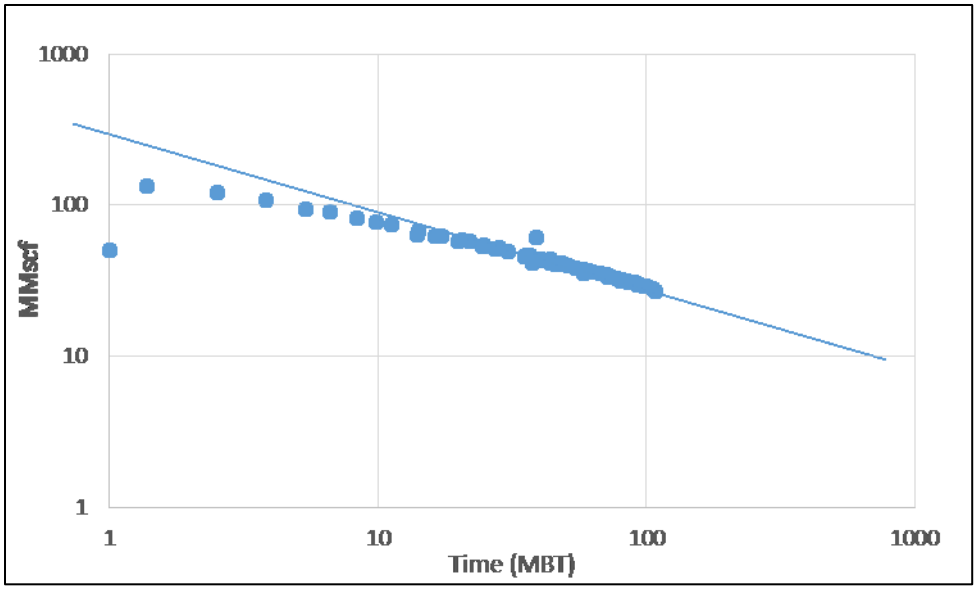

Fig. 20—Log-log plot, Rate vs. MBT, Well D

Fig. 20 shows, from a half-slope trend line, that Well D remains in transient linear flow for the entirety of the 60 months of publically available production data (and the duration for which we generated our forecasts). With this information, we generate production forecasts using our methods, extending the period for which we transient linear flow occurs for the 60 months forecasting duration period, in **Fig. 23.**

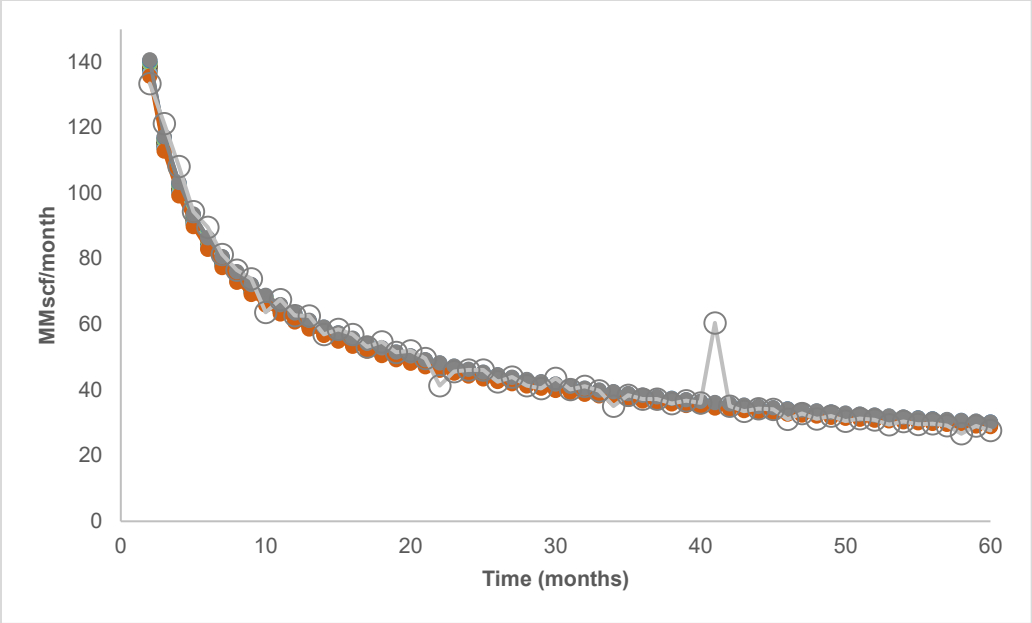

Fig. 21—Well D, 12-month history match and forecasts, months 0-60

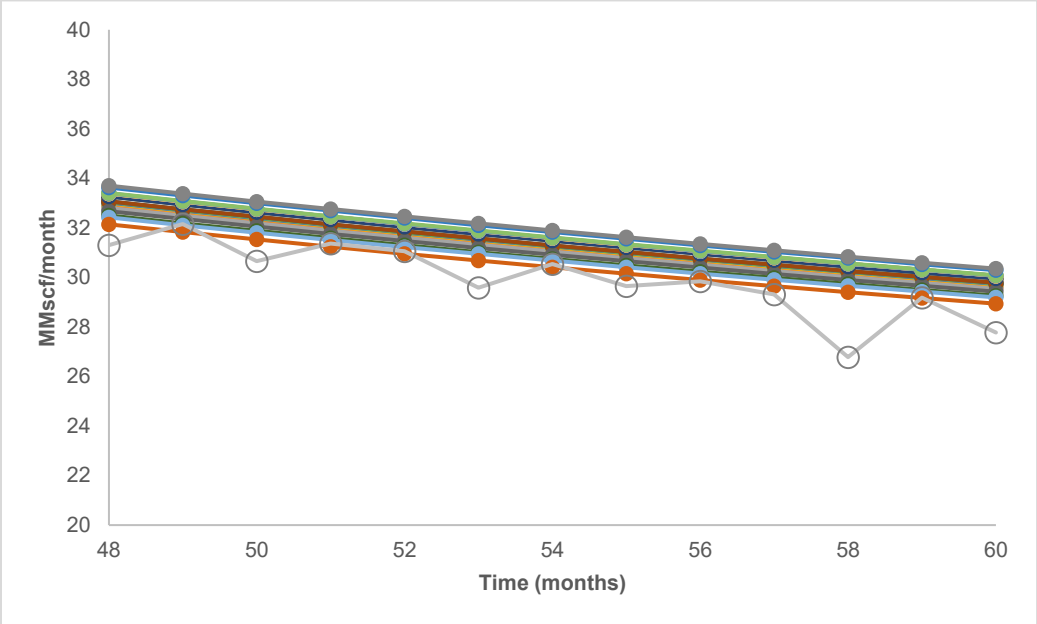

Fig. 22—Well D, 12-month history match and forecasts, months 48-60

Table 4 outlines the average absolute discrepancy between each generated forecast, and the monthly production rates of Well D, as well as the discrepancy between each trial's 12-month EUR and 60-month EUR when compared with the true EURs of Well D at those time durations.

Table 4—Quality of matches – 12-month history match, Well D

Run	12-month EUR discrepancy	60-month EUR discrepancy	12-month Average ABS Rate discrepancy	60-month Average ABS Rate discrepancy
227	2.75%	1.19%	5.21%	2.60%
231	2.75%	1.19%	5.21%	2.60%
880	2.38%	0.86%	4.96%	2.59%
682	1.70%	0.24%	4.52%	2.58%
941	1.62%	0.18%	4.48%	2.60%
447	1.32%	-0.10%	4.32%	2.72%
108	0.81%	-0.56%	4.08%	2.94%
119	0.81%	-0.56%	4.08%	2.94%
1167	0.61%	-0.74%	3.99%	3.03%
1413	-0.03%	-1.32%	3.74%	3.31%
678	-0.07%	-1.36%	3.73%	3.33%
641	-0.09%	-1.37%	3.72%	3.34%
652	-0.09%	-1.37%	3.72%	3.34%
669	-0.09%	-1.37%	3.72%	3.34%
1104	-0.42%	-1.67%	3.62%	3.50%
1126	-0.42%	-1.67%	3.62%	3.50%
1433	-0.96%	-2.17%	3.53%	3.83%
719	-0.96%	-2.17%	3.53%	3.83%
1372	-1.05%	-2.24%	3.52%	3.88%
628	-1.12%	-2.30%	3.51%	3.92%
863	-1.18%	-2.36%	3.51%	3.96%
365	-1.48%	-2.64%	3.51%	4.14%
975	-1.72%	-2.85%	3.51%	4.29%
430	-2.08%	-3.18%	3.51%	4.51%
900	-2.58%	-3.63%	3.55%	4.81%
195	-2.80%	-3.83%	3.58%	4.94%
852	-3.58%	-4.54%	3.80%	5.42%
426	-3.79%	-4.73%	3.90%	5.55%
389	-3.81%	-4.75%	3.90%	5.56%
400	-3.81%	-4.75%	3.90%	5.56%
417	-3.81%	-4.75%	3.90%	5.56%
1256	-4.05%	-4.97%	4.03%	5.71%
1474	-4.23%	-5.14%	4.13%	5.82%
1502	-4.23%	-5.14%	4.13%	5.82%
611	-4.57%	-5.45%	4.33%	6.03%
376	-4.80%	-5.65%	4.47%	6.17%
1092	-4.89%	-5.74%	4.52%	6.22%
1338	-5.07%	-5.91%	4.64%	6.34%
1444	-5.09%	-5.92%	4.65%	6.35%
113	-5.50%	-6.29%	4.91%	6.59%
Average	**-1.59%**	**-2.74%**	**4.03%**	**4.33%**

The treatment combinations of input parameters which yielded the seven best-fit forecasts to Well D based on a 12-month history match are listed in Section 3.3, in **Table 11**.

The production forecasts generated on the basis of a 12-month history for Well D match true production data sufficiently well (when we have foresight to when t_{elf} will actually occur), estimating monthly rates within 5%, 12-month EUR within 2%, and 60-month EUR within 3%.

We then investigate how the fit of rate-time profiles could be improved for Well D, when generated on the basis of a 60-month history match.

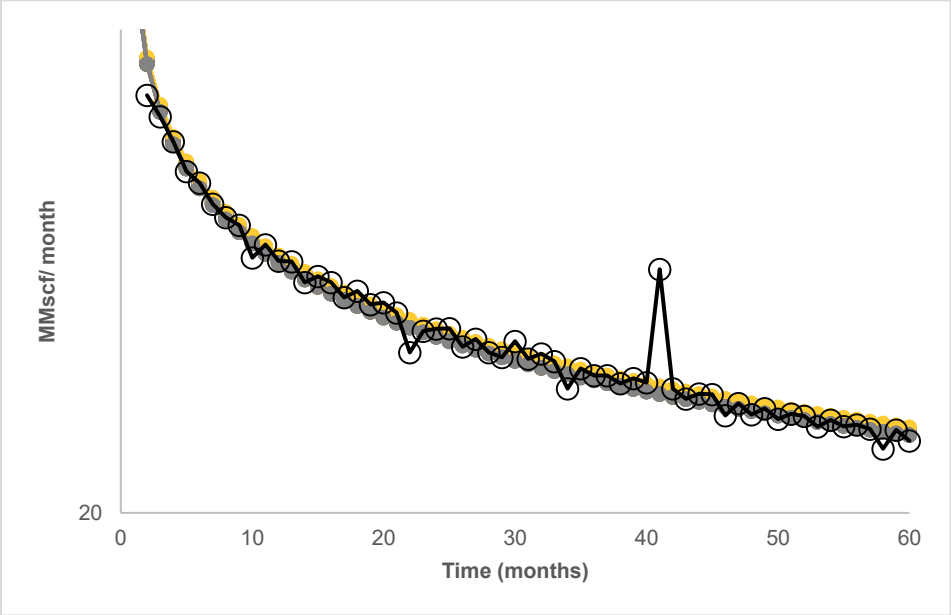

Fig. 23—Well D, 60-month history match rate-time profiles, months 0-60

In **Fig. 24** through **Fig. 26**, we parse this forecast into smaller time increments, to analyze more closely the quality of the 60-month history match forecasts.

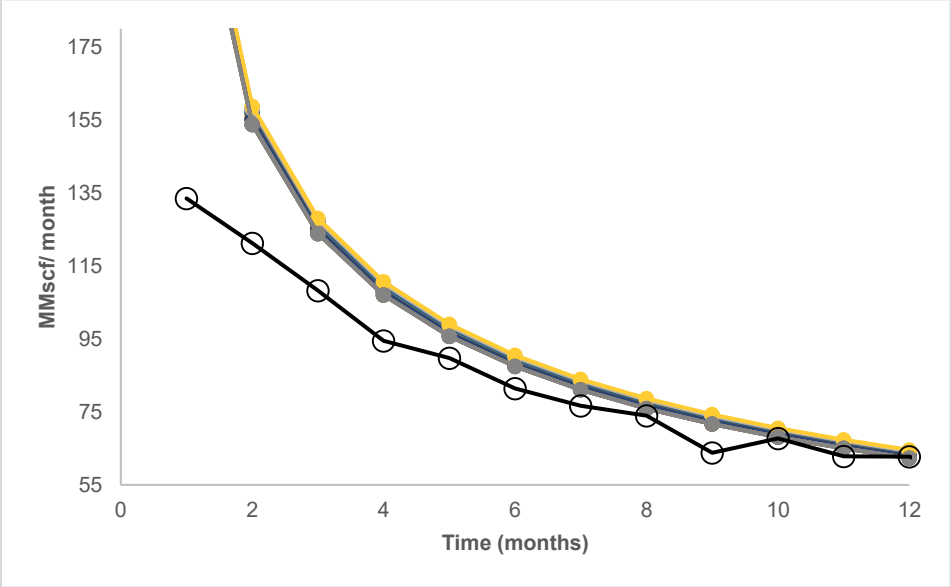

Fig. 24—Well D, 60-month history match rate-time profiles, months 0-12

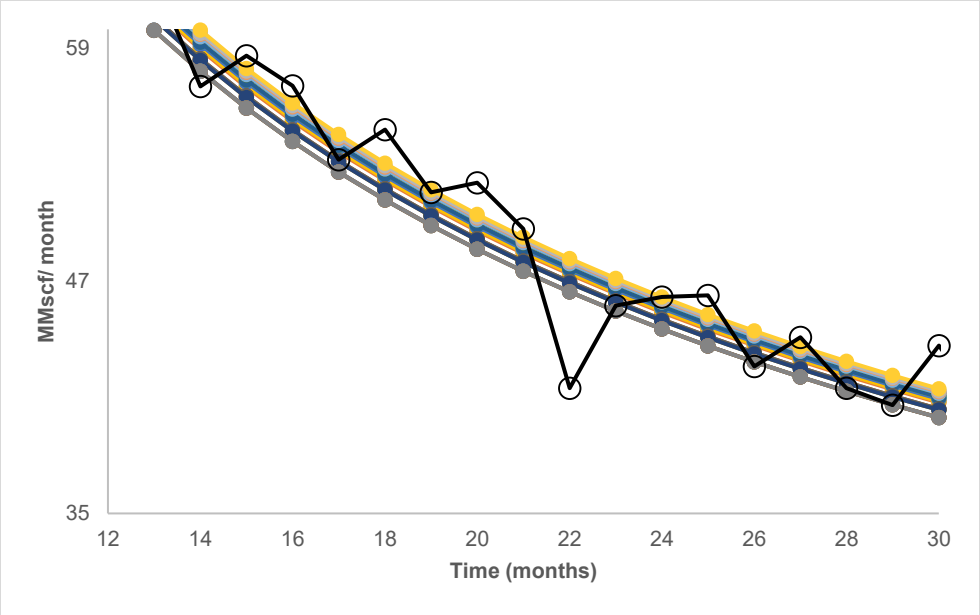

Fig. 25—Well D, 60-month history match rate-time profiles, months 12-30

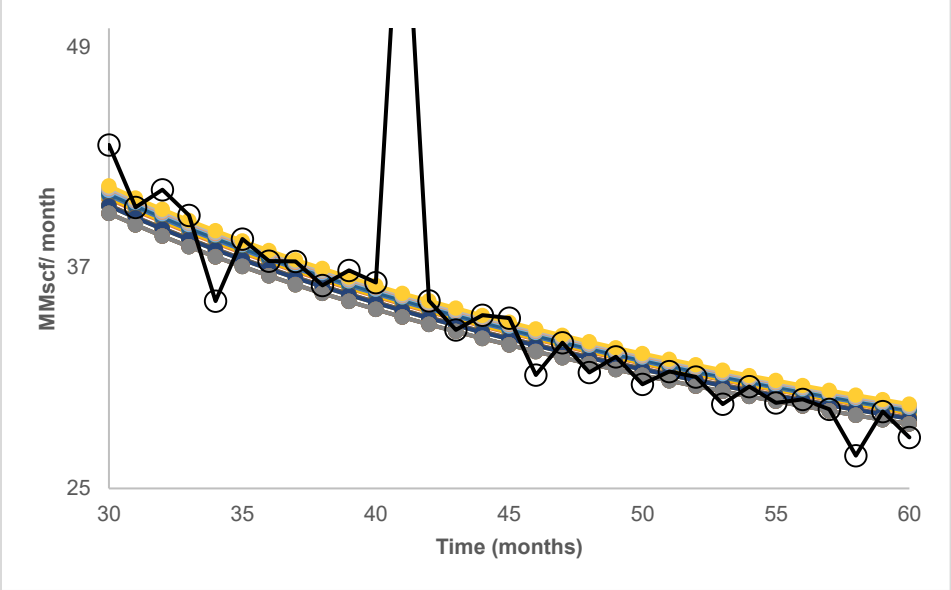

Fig. 26—Well D, 60-month history match and forecasts, months 30-60

The 40 best-fit history matches, shown in Fig. 24 through Fig. 26 (matched on 60 months of production data), match the true production data of Well D satisfactorily for months 0-60: each of the 40 best-fit rate-time profiles for Well D estimate monthly production rates within less than 4% discrepancy (**Table 5**). We conclude that having more production history as a basis to history match yields better fitting production forecasts when using our proposed workflow, although this is no surprise. This is correlated with having a better understanding of when t_{elf} will occur; while we vary this parameter with DOE techniques, history matching for other reservoir and completion parameters simultaneously, t_{elf} could also be estimated using the equation presented in (12), in combination with (3), presented by Wattenbarger (by history matching available production data). Proper estimation of t_{elf} is critical when trying to properly forecast production for longer periods of time.

Table 5 outlines the average absolute discrepancy between the production rates of Well D, and the 40 best-fit rate-time profiles (generated based on a 60-month history match) as well as the discrepancy between each trial's 12-month EUR and 60-month EUR when compared with the true EURs of Well D at those time durations.

Table 5— Quality of matches: 60-month history match, Well D

Run	12-month EUR discrepancy	60-month EUR discrepancy	60-month Average ABS rate discrepancy
195	5.37%	5.36%	5.09%
1144	5.12%	5.12%	4.87%
426	3.98%	4.00%	3.95%
389	3.96%	3.99%	3.94%
400	3.96%	3.99%	3.94%
417	3.96%	3.99%	3.94%
1256	3.68%	3.72%	3.77%
1474	3.47%	3.51%	3.65%
1502	3.47%	3.51%	3.65%
611	3.07%	3.13%	3.46%
376	2.81%	2.88%	3.37%
1092	2.71%	2.77%	3.33%
1338	2.50%	2.57%	3.27%
1444	2.48%	2.55%	3.27%
113	2.01%	2.09%	3.15%
441	2.00%	2.08%	3.14%
1161	1.80%	1.89%	3.10%
648	1.52%	1.61%	3.06%
663	1.52%	1.61%	3.06%
178	1.35%	1.45%	3.04%
1403	0.54%	0.67%	3.05%
1407	0.54%	0.67%	3.05%
600	0.40%	0.53%	3.07%
622	0.40%	0.53%	3.07%
174	-0.54%	-0.39%	3.37%
148	-0.56%	-0.41%	3.38%
165	-0.56%	-0.41%	3.38%
1355	-0.56%	-0.41%	3.38%
1366	-0.56%	-0.41%	3.38%
359	-1.03%	-0.86%	3.60%
852	-1.50%	-1.32%	3.85%
215	-1.50%	-1.32%	3.85%
1302	-1.60%	-1.42%	3.91%
471	-1.66%	-1.48%	3.94%
909	-1.86%	-1.67%	4.05%
900	-2.44%	-2.24%	4.42%
185	-2.53%	-2.32%	4.48%
396	-2.75%	-2.54%	4.63%
868	-2.79%	-2.57%	4.66%
1222	-2.79%	-2.57%	4.66%
Average	0.93%	1.05%	3.68%

3.1.2 Identifying probabilistic forecasts for Well D, 12-month history match

While a range of forecasts as we have presented for Well D are valuable, assigning specific P10, P50, and P90 forecasts are of greater interest to industry, as these forecasts and estimates comply with both PRMS and SEC standards. Because operators typically will not have access to five years of production data (with which to history-match and generate production forecasts), we return to the forecasts generated with only 12 months of production data for Well D for this portion of work.

We then analyzed the best-fit cumulative production forecasts for Well D (generated on the basis of a 12-month history match): from these best-fit forecasts representative P10, P50, and P90 forecasts for Well D were determined, based on level of discrepancy from the reference solution (the true 12-month cumulative production of Well D). These forecasts were identified on the assumption that we know that boundary-dominated flow will not occur for this particular well during the period of time for which we are interested in (first 60 months of well life). This is confirmed by the log-log plot shown in Fig. 20.

We show the 12-month EURs for each of the best-fit forecasts, arranged in ascending order, according to the discrepancy from true 12-month EUR, in **Table 6**. Run 447 yields a forecast with a discrepancy closest to 0 (discrepancy of -.10%), which can logically be viewed as a P50 forecast (this is highlighted (in blue) in Table 6). By fitting the 12-month EUR discrepancies shown in Table 4 with a normal probability distribution with a mean of -.10%, P90 and P10 discrepancies, and corresponding P90 and P10 forecasts, can be identified: Run 1388 and Run 231 were determined as P90 and P10 forecasts, respectively, and are also highlighted in Table 6 (in green, and in

orange, respectively). Trials which yielded duplicate 12-month EURs and 12-month EUR discrepancies are not shown in this table. These results yield a considerably small P10/P90 ratio of 1.07, indicating an estimated range of outcomes that may be overly confident.

Table 6— Comparing 12-month EURs: Well D

Run	12-month EUR discrepancy	12-month EUR (MMscf)
227	1.19%	1049
231	1.19%	1049
880	0.86%	1045
682	0.24%	1039
941	0.18%	1038
447	-0.10%	1035
108	-0.56%	1031
1167	-0.74%	1029
1413	-1.32%	1023
678	-1.36%	1022
669	-1.37%	1022
1104	-1.67%	1019
1433	-2.17%	1014
1372	-2.24%	1013
628	-2.30%	1013
863	-2.36%	1012
365	-2.64%	1009
975	-2.85%	1007
430	-3.18%	1003
900	-3.63%	999
195	-3.83%	997
852	-4.54%	989
426	-4.73%	987
417	-4.75%	987
1256	-4.97%	985
1474	-5.14%	983
611	-5.45%	980
376	-5.65%	978
1092	-5.74%	977
1338	-5.91%	975
1444	-5.92%	975
113	-6.29%	971

The representative P10, P50, and P90 forecasts, based on discrepancy from 12-month EUR, as well as the reference solution, is shown in **Fig. 27**.

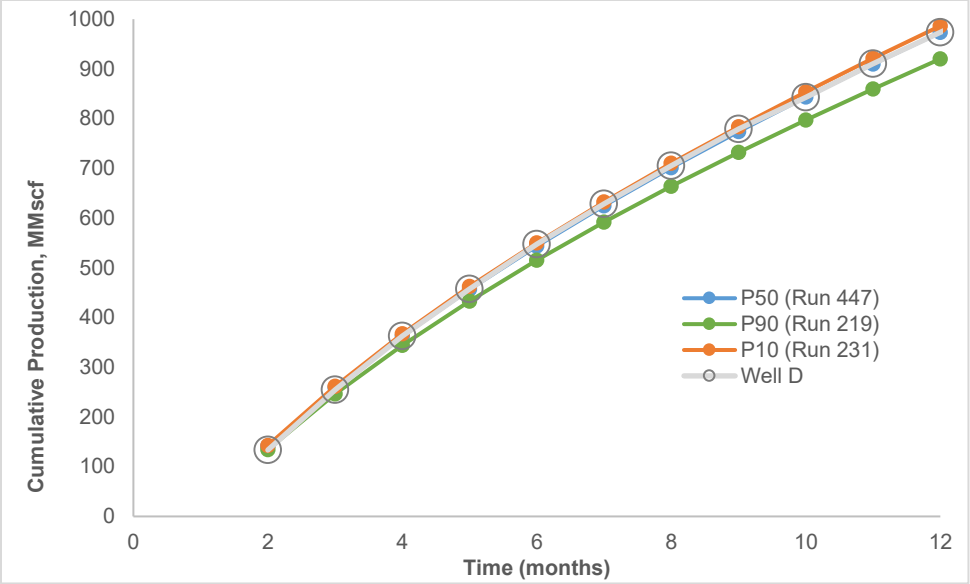

Fig. 27— Comparison of 12-month cumulative gas production forecasts: Well D, 12-month history match

Although the forecasts were generated on a 12-month history match, we then expand these forecasts to assess how they look after 60 months, analyzing the quality more closely, by focusing on the last 20 months of the 60-month forecasting period, in **Fig. 28.**

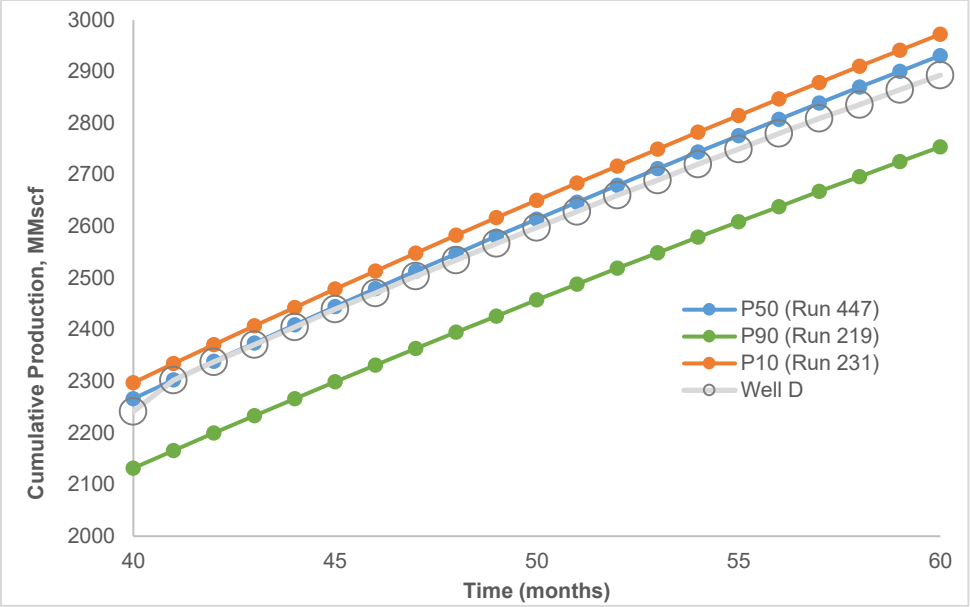

Fig. 28— Comparison of 60-month cumulative gas production forecasts (months 40-60): Well D, 12-month history match

We can see from Fig. 27 and Fig. 28 that the methods we present can be used to quickly, easily—but most importantly—sufficiently probabilistically forecast production, despite limited available production data used to history match and forecast production for Well D.

The forecasts, when extrapolated to 60 months, yield a 60-month P10/P90 ratio of 1.08, also narrow. A narrow range such as this is not always preferable or appropriated when evaluating many different scenarios. In upcoming sections, we assess the validity of this narrow band of estimated forecasts, and discuss using a decreased number of experimental runs when history matching production to obtain a wider range of forecasts.

3.1.3 Forecasting production for Well K, 12-month history match and 60-month history match

We then perform the same series of history matches for Well K, as we had done for Well D. When looking at the gas normalized pressure vs. $\sqrt{t}$ plot of Well K (shown in Fig. 29), to determine the m_{cpT}, and intercept (b'), we can see that the values of m_{cpT} and b' differ significantly when matched with either 12, 24, or 60 months of production data.

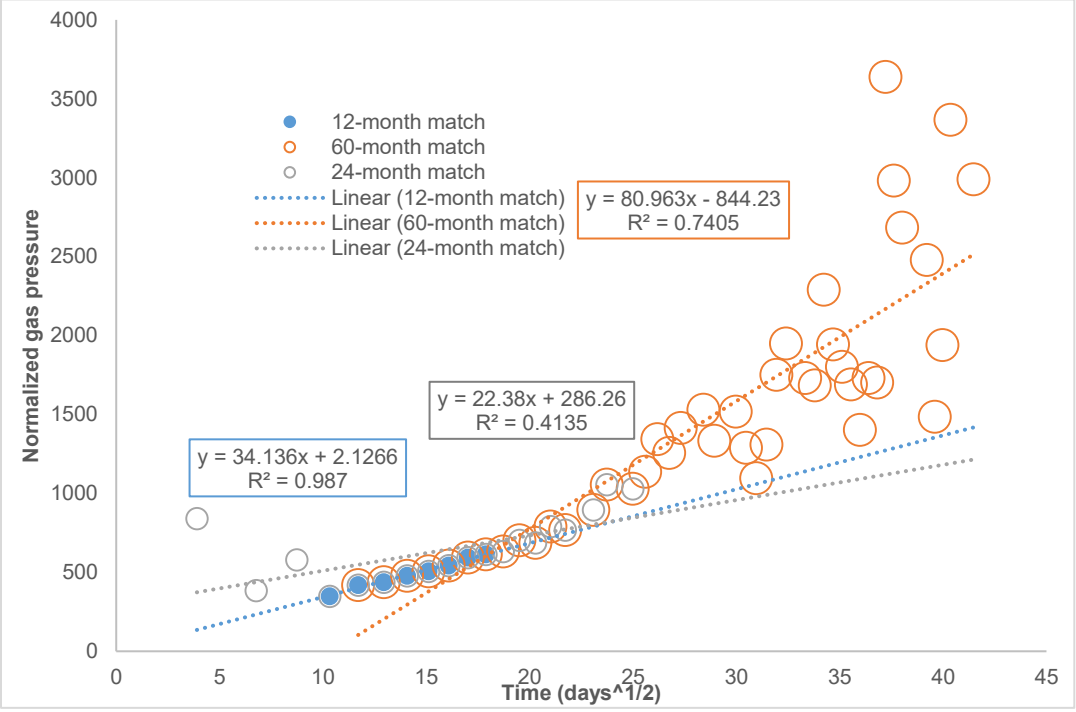

Fig. 29— Assessing m_{cp}: Well K

From Fig. 29, it is clear that unlike Well D (shown in Fig. 16), m_{cp} (and *b'* intercept) change considerably from an analysis of 12 months of production data, when compared with parameters drawn from a diagnosis of 24 months or 60 months of production data.

For this portion of work, we systematically vary four parameters, fracture half-length (x_f), porosity (φ), formation height (h), and permeability (k), using DOE techniques (and using the same 1,000 treatment combinations used for Well D) for the history matching portion of our workflow. Using the 1,000 treatment combinations, and with known parameters of Well K (number of fractures, n_f, initial pressure, p_i), assumed parameters of Well K (flowing well pressure, p_{wf},) and estimated parameters of Well K (pseudo-pressures, total compressibility, c_t, and viscosity, μ) 1,000 m_{cp} values were calculated for Well K.

These treatment combinations were then ranked based on how closely their calculated m_{cp} values matched the target $m_{cp\underline{T}}$ value of Well K (determined from the diagnostic plot shown in Fig. 29, using the 12-month production data and trend line). The m_{cp} values which most closely matched the $m_{cp\underline{T}}$ value of Well K were then used to generate production forecasts during the transient flow period. As mentioned in Chapter 2, an independent method is needed to forecast production during BDF: for every best-matched treatment combination, a unique t_{elf} and D_i will be estimated, and a b-parameter of .4 will be used to estimate production in BDF using Arps' decline relations.

In **Fig. 30**, we show 40 best-fit forecasts (when history matched with a 12-month m_{cpT}), for Well K.

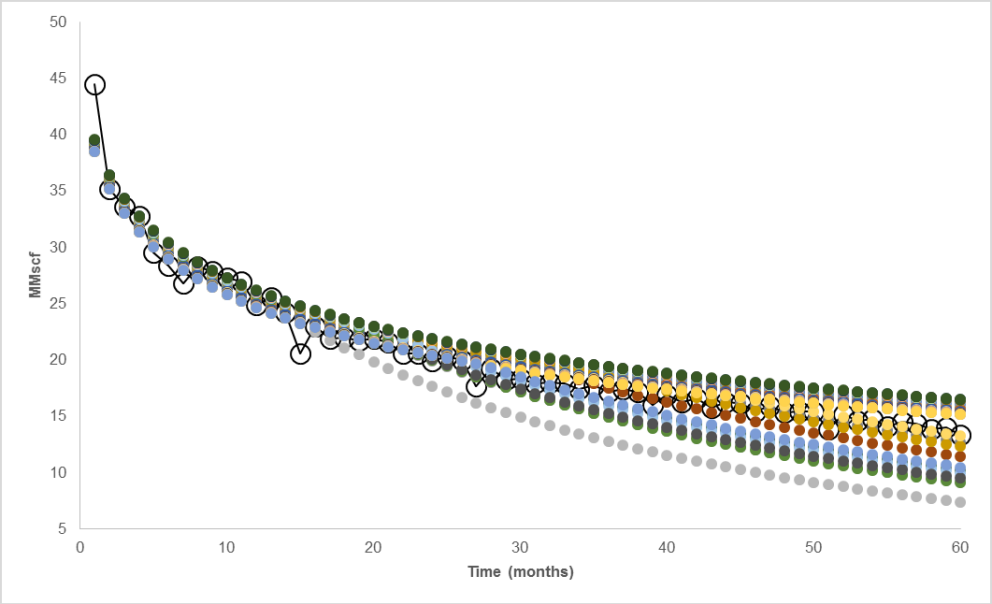

Fig. 30—Well K, 12-month history match and forecasts

In **Fig. 31** and **Fig. 32**, we parse this forecast into smaller time increments, to analyze the quality of the forecasts generated on the basis of a 12-month history match, more closely.

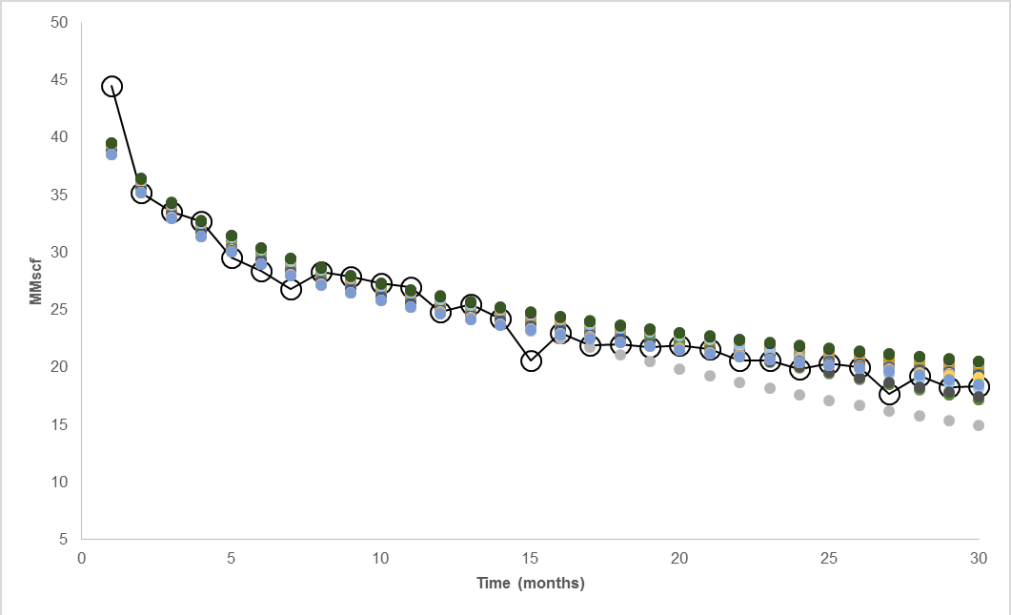

Fig. 31—Well K, 12-month history match and forecasts, months 0-30

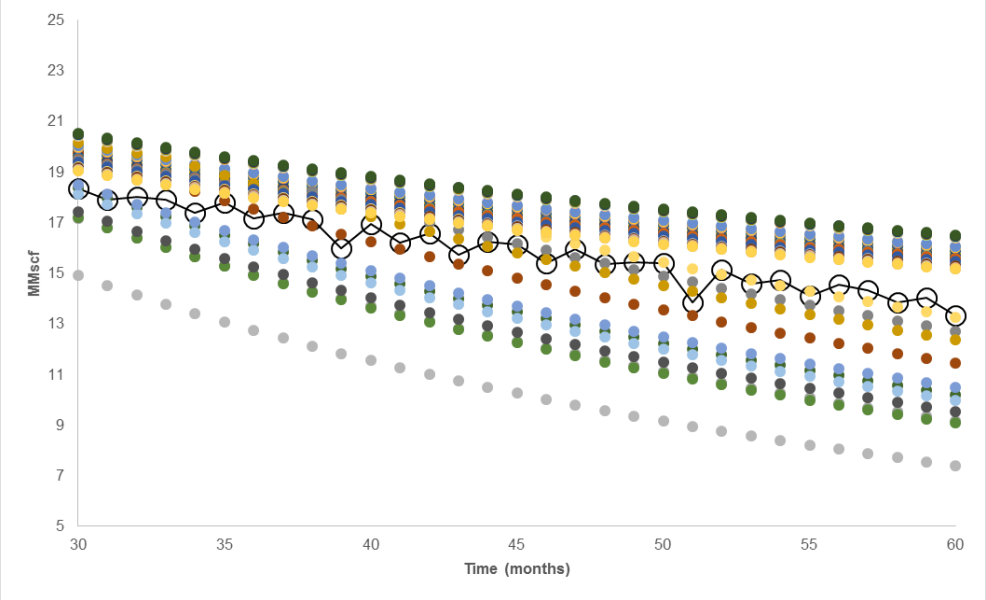

Fig. 32—Well K, 12-month history match and forecasts, months 30-60

The forecasts shown in Fig. 31 and Fig. 32, match the true production data of Well K satisfactorily for months 0-60, when history-matched with only 12 months of production data. **Table 7** outlines the average absolute discrepancy between each generated forecast, and the monthly production rates of Well K, as well as the discrepancy between each trial's 12-month EUR and 60-month EUR when compared with the true EURs of Well K at those time durations. Recall that each of the forecasts reviewed in this table switch to forecasting in BDF at different times, in accordance with the values of the parameters within the treatment combination used to history match and generate the forecast.

Table 7—Quality of matches – 12-month history match, Well K (variable t_{elf})

Run	12-month EUR discrepancy	60-month EUR discrepancy	12-month Average ABS rate discrepancy	60-month Average ABS rate discrepancy
1310	-3.19%	1.38%	3.29%	3.66%
91	-3.19%	-15.57%	3.29%	19.93%
1291	-3.12%	1.98%	3.26%	4.50%
1028	-3.04%	1.94%	3.23%	4.32%
1045	-3.04%	1.94%	3.23%	4.32%
883	-2.99%	-17.76%	3.38%	22.55%
801	-2.82%	0.44%	3.16%	3.00%
829	-2.82%	0.44%	3.16%	3.00%
57	-2.73%	-2.07%	3.13%	4.90%
1357	-2.73%	-8.16%	3.13%	11.40%
68	-2.14%	-1.84%	3.03%	5.51%
1094	-1.86%	-8.98%	3.00%	12.86%
256	-1.75%	2.55%	2.99%	3.86%
583	-1.72%	1.30%	2.99%	3.55%
1327	-1.69%	3.62%	2.99%	5.32%
1053	-1.41%	3.17%	2.96%	4.38%
1081	-1.41%	3.17%	2.96%	4.38%
782	-1.39%	4.12%	2.96%	5.80%
343	-1.37%	-11.65%	2.96%	16.14%
1135	-1.24%	-14.62%	2.88%	19.55%
391	-1.06%	-16.70%	2.76%	21.98%
169	-0.97%	-18.13%	3.63%	23.83%
38	-0.94%	2.95%	2.96%	4.07%
309	-0.92%	1.75%	2.96%	4.16%
1023	-0.58%	5.63%	2.98%	7.35%
1280	-0.49%	5.92%	2.98%	7.73%
1297	-0.49%	5.92%	2.98%	7.73%
818	-0.20%	4.36%	3.00%	5.11%
835	-0.20%	4.36%	3.00%	5.11%
536	-0.10%	5.64%	3.00%	6.91%
1034	0.01%	6.52%	3.01%	8.16%
595	0.28%	-7.96%	3.03%	13.06%
643	0.54%	-13.60%	3.02%	18.99%
128	0.69%	-15.08%	3.15%	20.86%
1333	1.11%	7.87%	3.23%	9.22%
1070	1.20%	7.12%	3.26%	8.01%
1087	1.20%	7.12%	3.26%	8.01%
572	1.31%	5.87%	3.31%	6.14%
760	1.40%	8.86%	3.37%	10.51%
16	1.49%	6.65%	3.45%	7.10%
Average	**-2.23%**	**-3.40%**	**3.08%**	**8.80%**

When history-matching (and forecasting) on only 12 months of production data, we have little inclination of when exactly the transition from transient flow to BDF will occur; it can be seen from Fig. 31 and Fig. 32 that some best-fit forecasts (best-fit to 12 months of production data) may not capture this transition time properly. To analyze to how many treatment combinations did yield an estimated t_{elf} consistent with true t_{elf} of Well K, we show a log-log plot of rate vs. MBT for Well K, in **Fig. 33.**

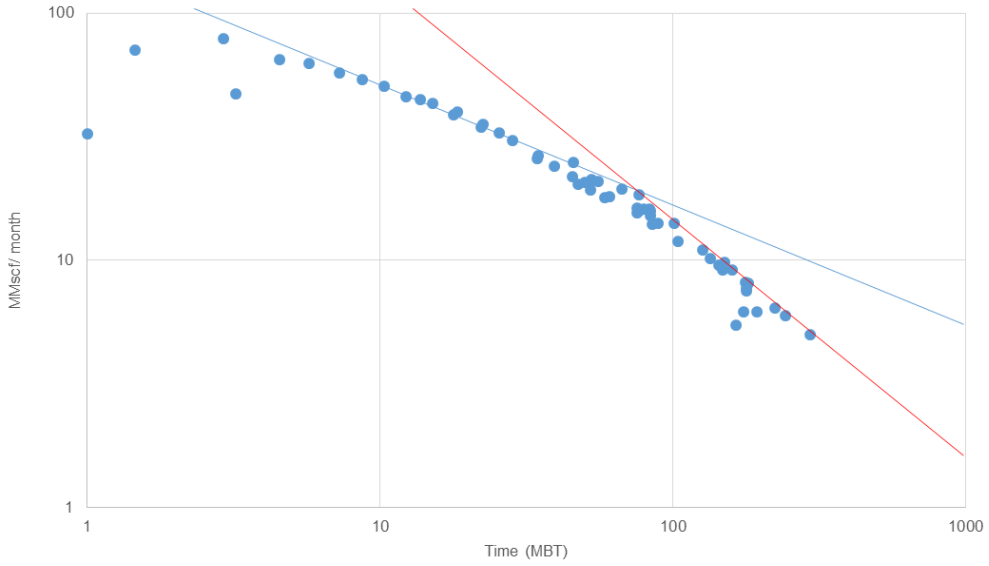

Fig. 33—Log-log plot, Rate vs. MBT, Well K

Fig. 33 shows, from a half-slope trend line, that Well K transitions into BDF between t ~ 33-34 months. With this information, we generate production forecasts using our methods, fixing the time at which we will switch to forecasting in BDF. We show these forecasts in **Fig. 34.**

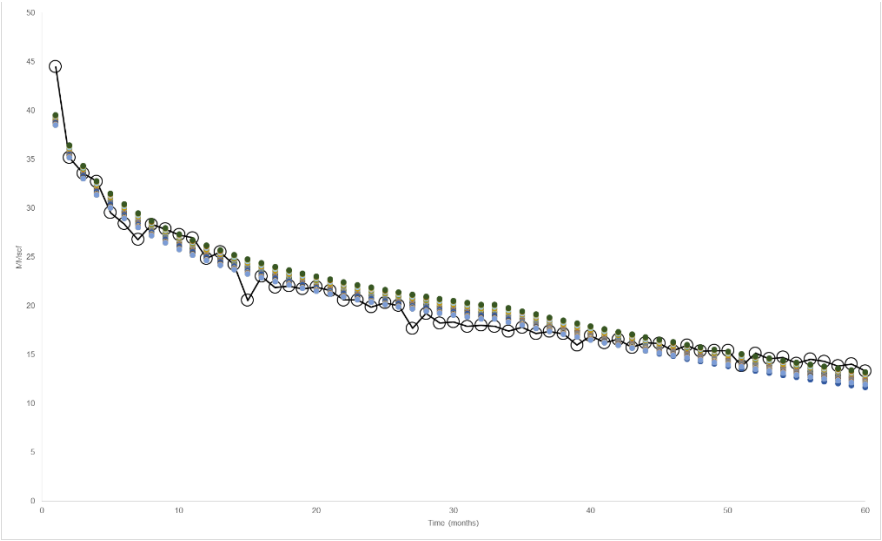

Fig. 34—Well K, 12-month history match and forecasts, months 0-60 (assumed t_{elf})

Comparing quality of fit of forecasts in Fig. 30 (12-month history match, no prevision of t_{elf}), and Fig. 34 (12-month history match, fixed t_{elf}) it is clear that quality of fit improves as more production data (and subsequent knowledge of t_{elf}) becomes available which again, is no surprise. **Table 8** outlines the average absolute discrepancy between each generated forecast, and the monthly production rates of Well K, as well as the discrepancy between each trial's 12-month EUR and 60-month EUR when compared with the true EURs of Well K at those time durations. Recall that each of the forecasts reviewed in this table switch to forecasting in BDF at a fixed time (33 months).

Table 8—Quality of matches – 12-month history match, Well K (fixed t_{elf})

Run	12-month EUR discrepancy	60-month EUR discrepancy	12-month Average ABS rate discrepancy	60-month Average ABS rate discrepancy
1310	-1.94%	-3.19%	3.29%	4.31%
91	-1.94%	-3.19%	3.29%	4.31%
1291	-1.84%	-3.12%	3.26%	4.28%
1028	-1.72%	-3.04%	3.23%	4.24%
1045	-1.72%	-3.04%	3.23%	4.24%
883	-1.41%	-2.82%	3.16%	4.17%
801	-1.41%	-2.82%	3.16%	4.17%
829	-1.41%	-2.82%	3.16%	4.17%
57	-1.28%	-2.73%	3.13%	4.15%
1357	-1.28%	-2.73%	3.13%	4.15%
68	-1.24%	-2.14%	3.03%	5.02%
1094	0.01%	-1.86%	3.00%	4.10%
256	0.17%	-1.75%	2.99%	4.10%
583	0.22%	-1.72%	2.99%	4.10%
1327	0.27%	-1.69%	2.99%	4.11%
1053	0.68%	-1.41%	2.96%	4.15%
1081	0.68%	-1.41%	2.96%	4.15%
782	0.71%	-1.39%	2.96%	4.16%
343	0.74%	-1.37%	2.96%	4.16%
1135	0.68%	-1.41%	2.96%	4.15%
391	1.42%	-0.92%	2.96%	4.29%
169	2.64%	-0.10%	3.00%	4.58%
38	1.38%	-0.94%	2.96%	4.28%
309	1.42%	-0.92%	2.96%	4.29%
1023	1.93%	-0.58%	2.98%	4.40%
1280	2.05%	-0.49%	2.98%	4.43%
1297	2.05%	-0.49%	2.98%	4.43%
818	2.50%	-0.20%	3.00%	4.54%
835	2.50%	-0.20%	3.00%	4.54%
536	2.64%	-0.10%	3.00%	4.58%
1034	2.81%	0.01%	3.01%	4.62%
595	3.22%	0.28%	3.03%	4.75%
643	3.89%	0.73%	3.13%	5.00%
128	3.81%	0.67%	3.11%	4.97%
1333	4.48%	1.11%	3.23%	5.24%
1070	4.61%	1.20%	3.26%	5.30%
1087	4.61%	1.20%	3.26%	5.30%
572	4.78%	1.31%	3.31%	5.40%
760	10.17%	1.40%	3.37%	12.33%
16	5.06%	1.49%	3.45%	5.58%
Average	**-0.55%**	**-2.22%**	**3.09%**	**4.22%**

Comparing the results in Table 7 and Table 8, it is clear that the more production data available for a well yields forecasts with improved fits to true production. The results in Table 8 (when t_{elf} is fixed, or known) estimate monthly production rates

within less than 5% discrepancy, on average, over a 60-month period of time, and estimate 60-month cumulative production within 3%, on average. We conclude that having more production history as a basis to history match yields better fitting production forecasts when using our proposed workflow, although this is no surprise. This is correlated with having a better understanding of when t_{elf} will occur; having this information is critical when trying to properly forecast production for longer periods of time.

3.1.4 Identifying probabilistic forecasts for Well K, 20-month history match

Just as we had performed for Well D, we then analyzed the best-fit cumulative production forecasts for Well K.

The 40 best-fit forecasts of Well K (12-month history-match, variable t_{elf}) were analyzed to determine representative P10, P50, and P90 forecasts, based on discrepancy from 12-month EUR We show the 12-month EURs for each of the best-fit forecasts in Table 7. For this portion of the analysis, we ignore t=1 in efforts to smooth the data.

Table 9—Identifying Probabilistic Forecasts, Well K

Run	Discrepancy, 12-month cumulative production, months 2-12
128	-1.61%
1333	-1.61%
643	-1.54%
818	-1.45%
835	-1.45%
391	-1.42%
1327	-1.22%
1053	-1.22%
1045	-1.13%
883	-1.13%
583	-0.49%
68	-0.19%
801	-0.08%
829	-0.04%
1357	-0.01%
1280	0.29%
1297	0.29%
1034	0.31%
536	0.34%
169	0.48%
16	0.65%
782	0.70%
572	0.79%
760	0.82%
1070	1.18%
1087	1.27%
595	1.27%
1135	1.59%
343	1.59%
1081	1.69%
57	1.81%
91	2.10%
1310	2.37%
1291	2.54%
1028	2.99%
1094	3.08%
256	3.08%
309	3.20%
38	3.31%
1023	3.40%

From Table 9, we then determine representative P10, P50, and P90 forecasts, based on discrepancy from a 12-month EUR: run 1357 yields a forecast with a discrepancy closest to 0 (discrepancy of -.01%), which can logically be viewed as a P50 forecast (this is highlighted (in blue) in Table 9). By fitting the 12-month EUR discrepancies

shown in Table 9 with a normal probability distribution with a mean of -.01%, P90 and P10 discrepancies, and corresponding P90 and P10 forecasts, can be identified. Run 1333 and Run 91 were identified as P90 and P10 forecasts, respectively, and are also highlighted in Table 9. We show these forecasts in **Fig. 35**. Although the forecasts were generated on the basis of a 12-month history match, we then expand these forecasts to assess how they look after 60 months.

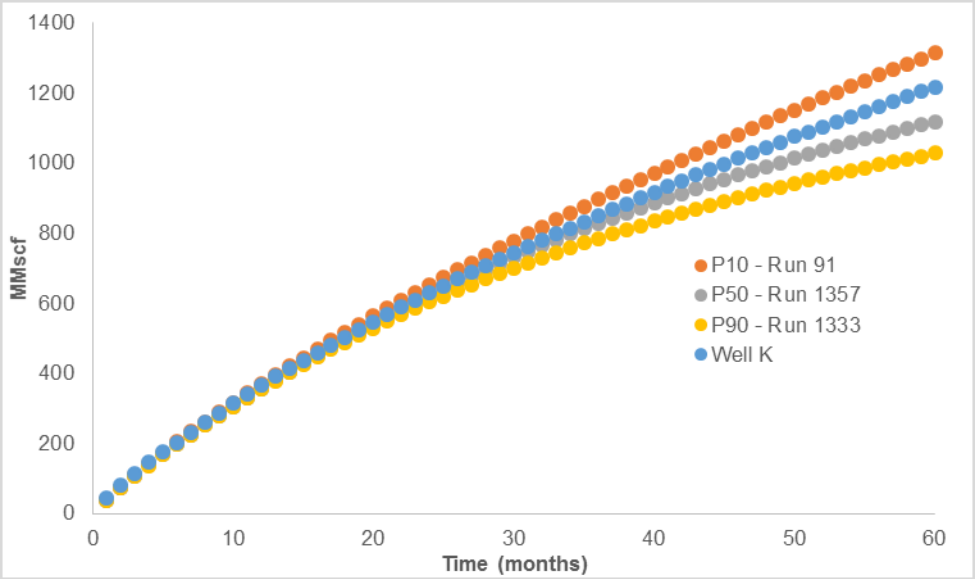

Fig. 35— Comparison of 60-month cumulative gas production forecasts: Well K, 12-month history match

We can see from Fig. 35 that even when t_{elf} is unknown, that the methods we present can be used to quickly, easily—but most importantly—sufficiently probabilistically forecast production, despite limited available production data used to history match and forecast production for Well K. The forecasts in Fig. 35 after 12 months, yield a

P10/P90 ratio of 1.05, and when extrapolated to 60 months, yield a 60-month P10/P90 ratio of 1.28.

As mentioned during the probabilistic forecasting of Well D, a narrow range such as this is not always preferable—or correct—when evaluating many different scenarios. In the following section, we validate this narrow band of Well D, and discuss using a decreased number of experimental runs when history matching production to obtain a wider range of forecasts.

3.1.5 Examples of application of method to history match and forecast production

We showcased Wells D and K in depth to show it is possible to achieve high-quality production forecasts using the methods we present, regardless of whether the well reaches BDF during the forecasting period. We use this section to review that our methods can be used to successfully history match available production data with treatment combinations generated with DOE techniques, and used to sufficiently forecast production in transient linear flow (followed by production in BDF if necessary) to generate a range of production forecasts, from which appropriate P10, P50, and P90 forecasts can be extracted. We show the true production of these wells and 20 best-fit history matches (history-matched from 12-15 months of available production data, depending on quality of data) and 60-month production forecasts, in **Fig. 36** through **Fig. 39.** All but one well shown in the below figures (Well I) is clearly shown to have reached BDF during the 60-month period forecasted when assessing a 60-month log-log rate vs. material balance time plot (MBT) plot. All log-log rate-MBT

plots for these wells (to detect transition from transient flow to BDF) are shown in **Fig. 55** through **Fig. 58** in the Appendix.

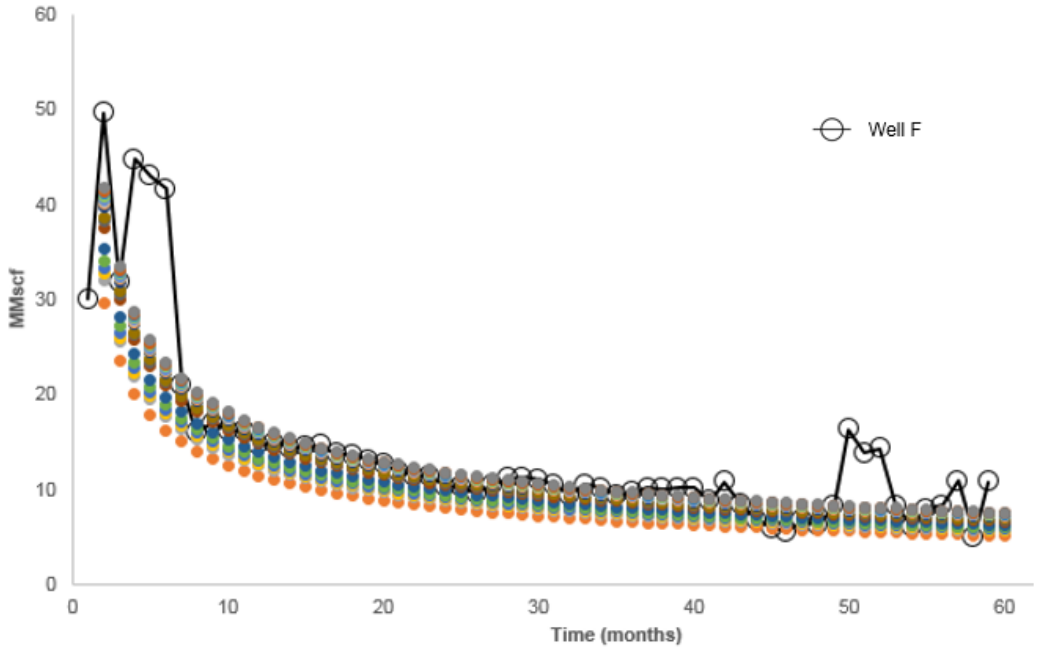

Fig. 36— Well F, 12-month history match and production forecasts

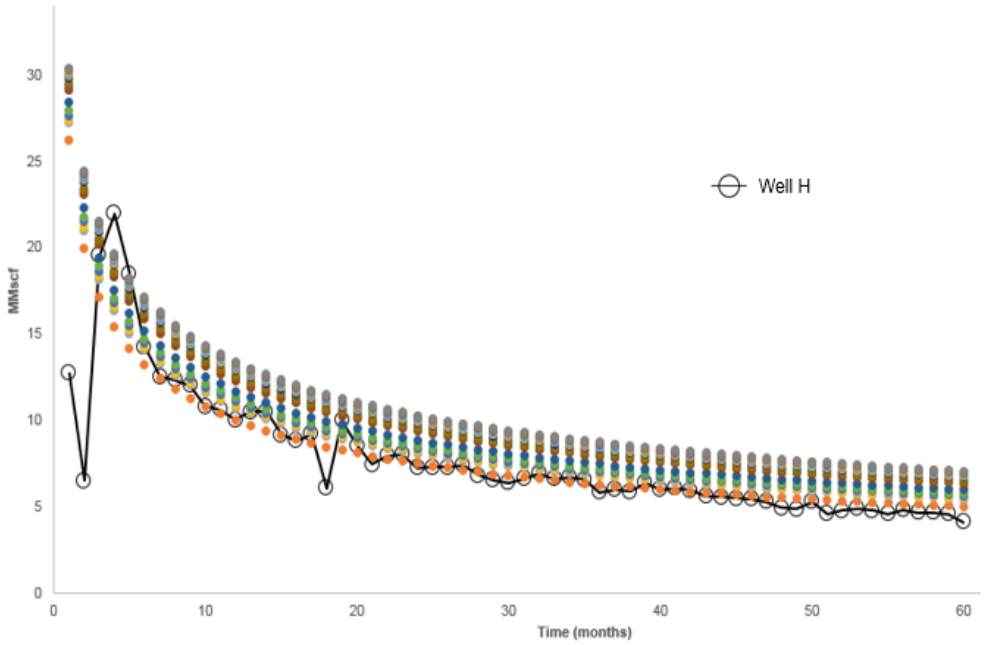

Fig. 37— Well H, 12-month history match and production forecasts

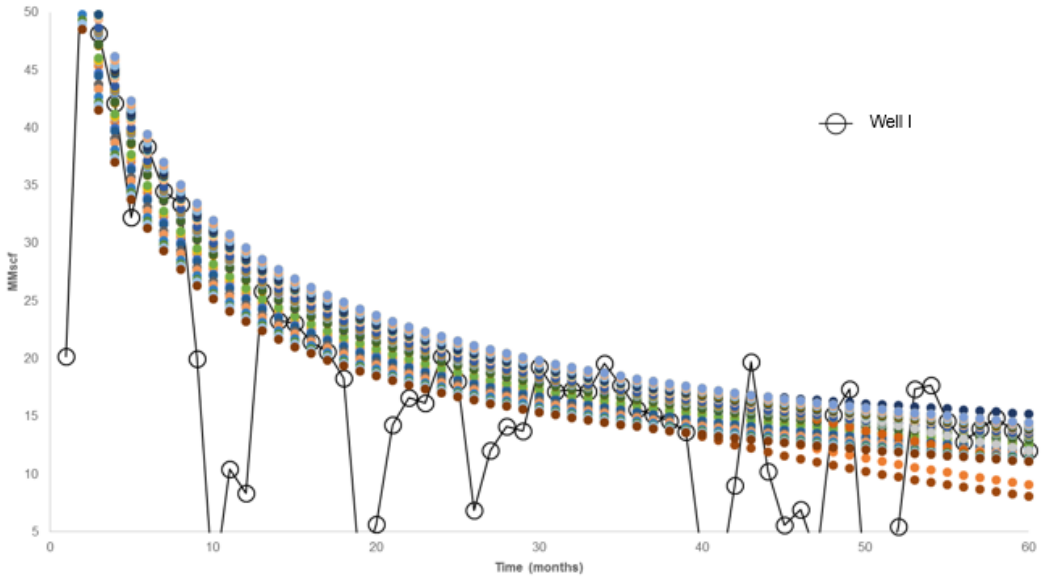

Fig. 38— Well I, 15-month history match and production forecasts

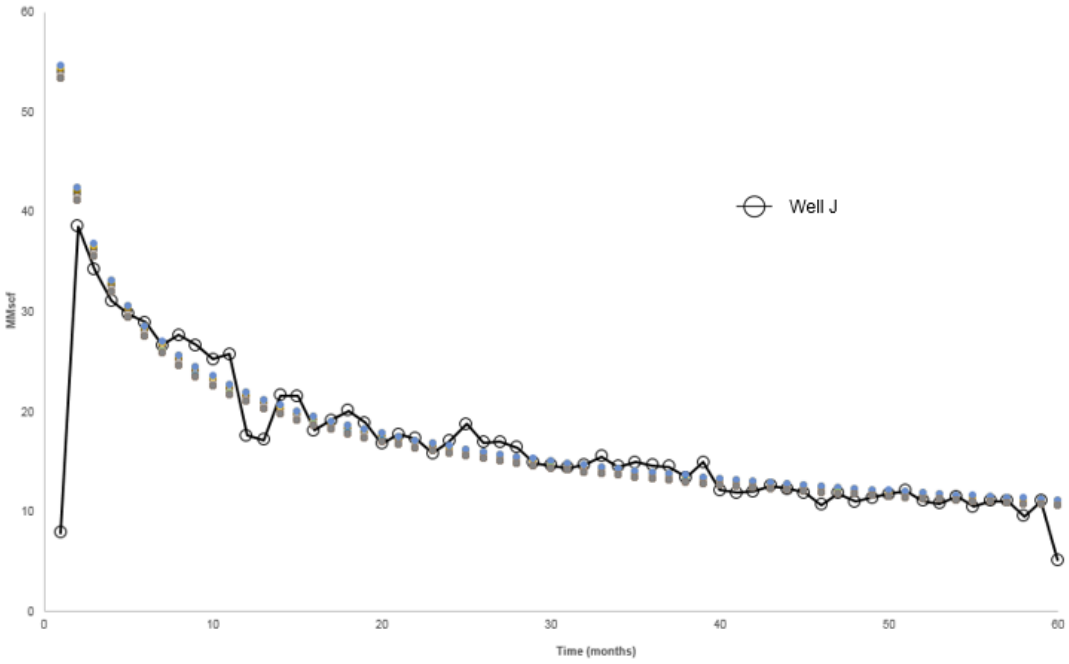

Fig. 39— Well J, 12-month history match and production forecasts

From the examples shown in Fig. 36 through Fig. 39, we show that when appropriate ranges of reservoir and completion parameters are sufficiently known, DOE techniques can be used to generate thousands of treatment combinations, from which a much more concentrated number of satisfactory history matches can be identified, and satisfactory production forecasts can be generated. Only 60 months of production data for each of the wells shown here is used to validate that forecasts generated, because only 60 months of production data was publically available for these wells. We validate how well this method can be used to forecast longer-term production in the following section.

3.1.6 Assessing reliability of methods to determine individual probabilistic forecasts

In this section, we assess the reliability of our methods in determining individual probabilistic forecasts by analyzing cumulative production levels, and P10/P90 ratios of nearly 120 MFHWs producing from the Barnett Shale.

The P10/P90 ratio is a useful performance metric in quantifying the variance of a given range of estimated production forecasts; a larger P10/P90 ratio indicates that dissimilar wells are being compared among a group, while a smaller P10/P90 ratio indicates a more homogenous group of wells: this homogeneity could be in reference to lateral length, net pay thickness, depth, and more (Ezisi et al. 2012).

We first assess the P10/P90 ratio of both 12-month cumulative production, and 60-month cumulative production for all 120 wells studied. The 12-month cumulative production of all 120 wells could be characterized by a lognormal distribution; we show this in a descending cumulative probability plot in **Fig. 40.** The 60-month cumulative production of all 120 wells could be characterized by a normal distribution; we show this in a descending cumulative probability plot in **Fig. 41.**

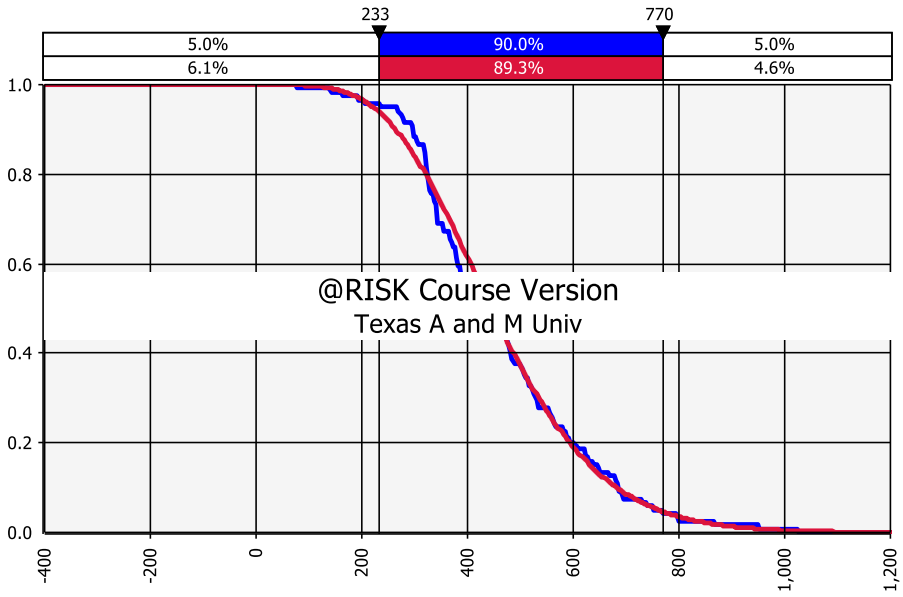

Fig. 40—12-month cumulative production, Barnett Shale MFHWs

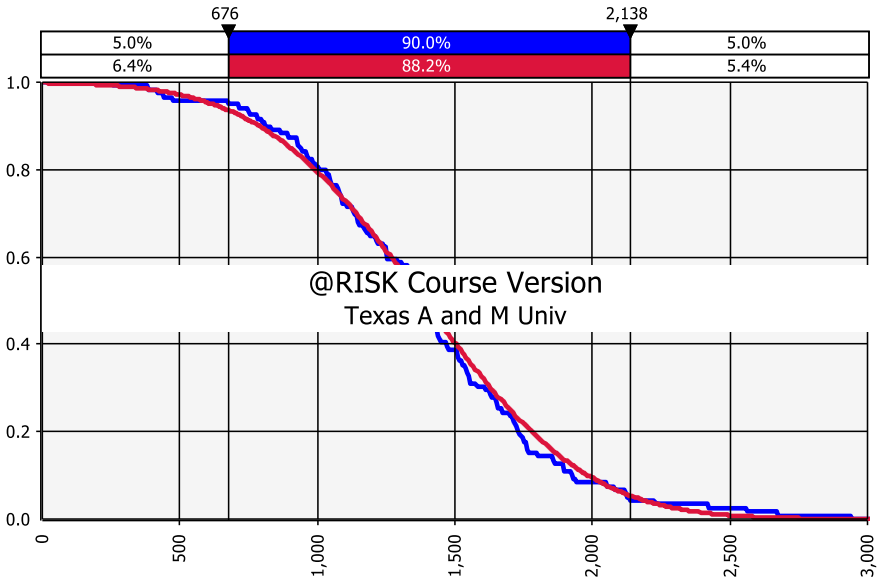

Fig. 41—60-month cumulative production, Barnett Shale MFHWs

Assessing 12-month cumulative production for all 120 wells studied yields a P10/P90 ratio of 2.31. Assessing 60-month cumulative production for all 120 wells studied also yields a P10/P90 ratio of 2.38. This is larger than the P10/P90 ratios we had calculated for Well D (1.07, 1.08), Well K (1.05, 1.28), and presumably larger than the P10/P90 ratios for other wells shown in Section 3.1.5. We mentioned previously that a very low P10/P90 ratio may be indicative of an estimated range of outcomes that is overly confident, and that this range should be wider when forecasting production (especially when limited production history is available).

We also discussed that the P10/P90 ratio is commensurate to the homogeneity of the group of wells being studied. To validate whether our narrow estimated ranges—when assessing whether production of Well D, Well K, and other wells we show in Section 3.1.5 are appropriate—we focus more closely on 16 wells from our 120 well data set which have very similar 12-month production volumes, all close to the average 12-month cumulative production of the entire set (462 MMscf).

Before assessing the P10/P90 ratios of this sample set, we first compare completion and reservoir characteristics of this 16-well sample against the completion and reservoir characteristics of the full set of wells. We compare the total vertical depth, the lateral lengths, and number of fracture stages between the two sets, in **Fig. 42**, **Fig. 43**, and **Fig. 44**, respectively.

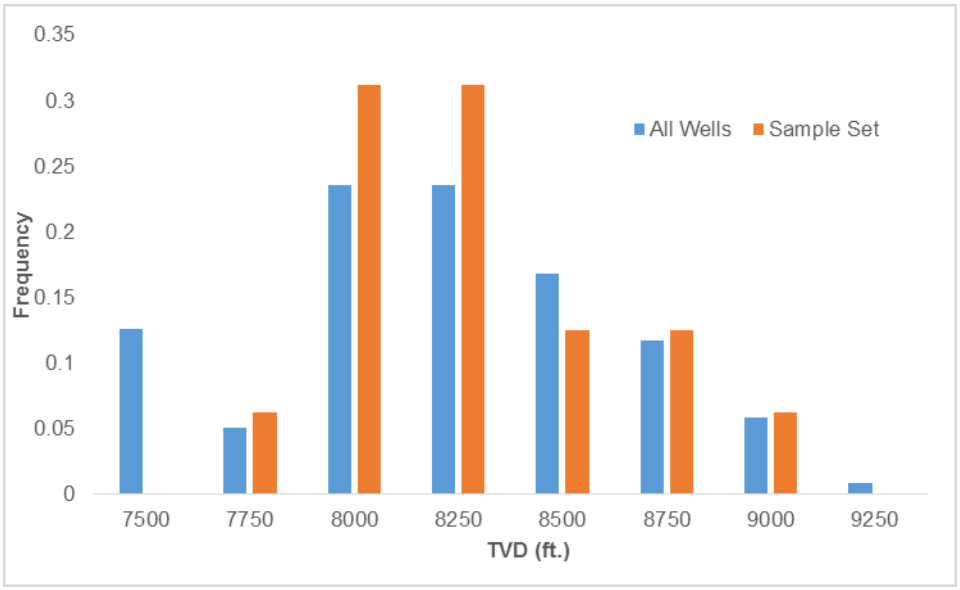

Fig. 42—Comparing relative frequency of TVD, Barnett Shale MFHWs

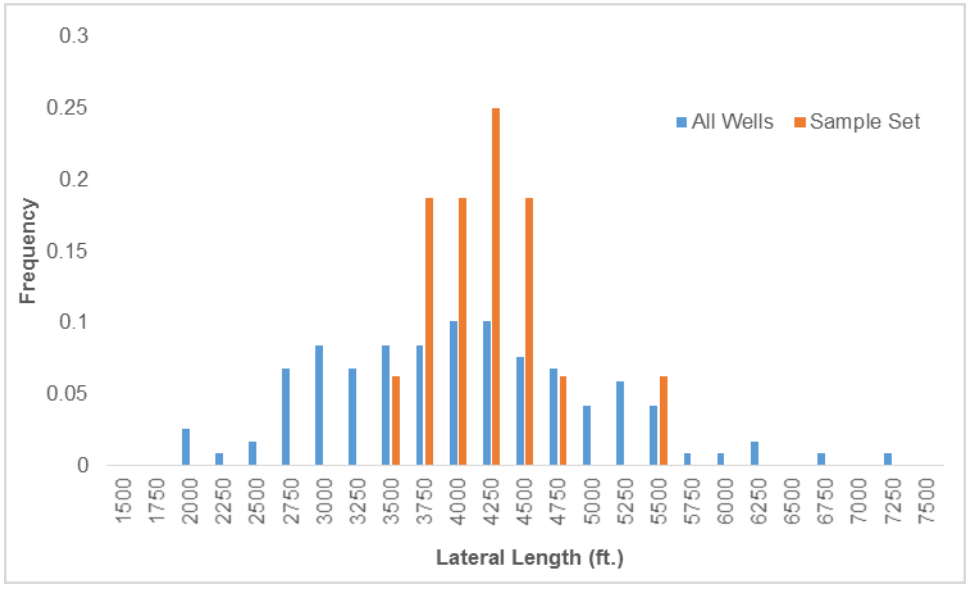

Fig. 43—Comparing relative frequency of Lateral Lengths, Barnett Shale MFHWs

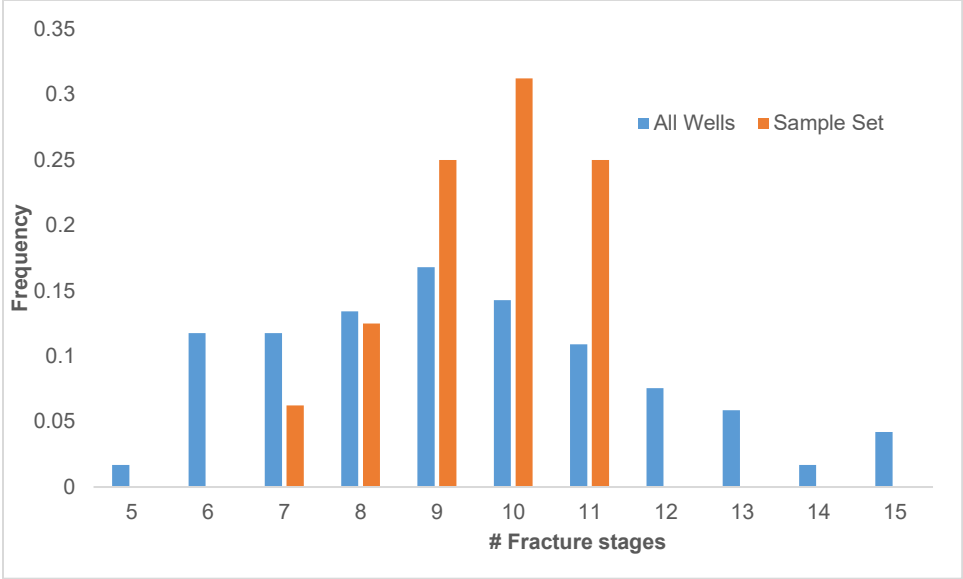

Fig. 44—Comparing relative frequency of fracture stages, Barnett Shale MFHWs

Fig. 42, Fig. 43, and Fig. 44 confirm that the subset of wells that we have chosen to analyze further when assessing P10/P90 ratios not only have similar 12-month cumulative production levels (ranging from 428 MMscf to 478 MMscf), these wells also have reservoir and completion characteristics that fall within a more concentrated range than when assessing all 120 wells. This homogeneity among wells in this subset would corroborate any smaller P10/P90 ratios, if they were to be observed.

The 12-month cumulative production of the sample set of wells could be best characterized by a uniform distribution; we show this in a descending cumulative probability plot in **Fig. 45**. The 60-month cumulative production of the sample set of wells could be best characterized by a triangular distribution; we show this in a descending cumulative probability plot in **Fig. 46**.

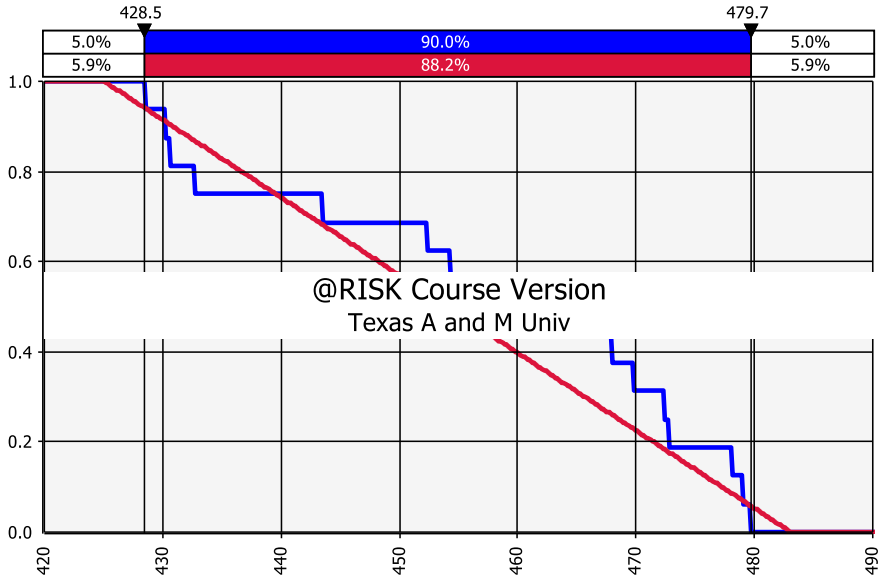

Fig. 45—12-month cumulative production, sample set, Barnett Shale MFHWs

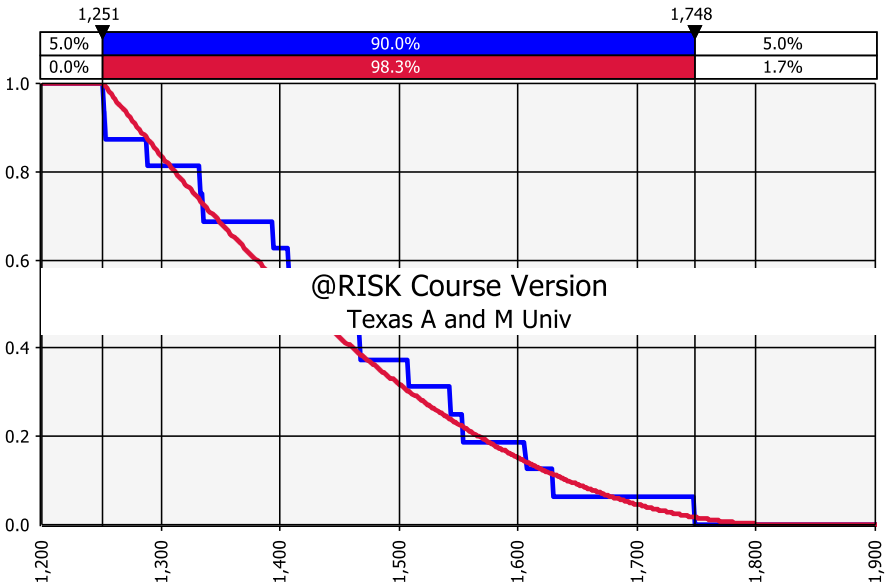

Fig. 46—60-month cumulative production, sample set, Barnett Shale MFHWs

Assessing 12-month cumulative production for this sample set of characteristically-similar (and prolifically-similar) wells yields a P10/P90 ratio of 1.11. Assessing 60-month cumulative production this sample set of wells studied yields a P10/P90 ratio of 1.31. These ratios are significantly smaller than the ratios we observe when assessing a much larger set of wells (of which have more variable completion and reservoir characteristics, as shown in Fig. 42 and Fig. 44). We conclude from this portion of work that P10/P90 ratios for wells of similar attributes have small P10/P90 ratios when comparing 12-month cumulative production levels, and 60-month cumulative production levels: when building probabilistic forecasts for individual wells, it would be appropriate to have P10/P90 ratios that are just as small—if not smaller than—the ratios we observe for a concentrated group of wells.

While the P10/P90 ratios of our probabilistic forecasts for Well D and Well K could be realistic, for risk-adverse planning purposes, the probabilistic ranges for these estimates could afford to be made wider. Because the purpose of DOE techniques is to survey the broad experimental space in the minimum number of runs, we suspected that had we performed the history-matching process on a decreased number of treatment combinations, that our P10/P90 ratios would be greater, and possibly more appropriate when determining P10, P50, and P90 forecasts. We show probabilistic forecasts identified from pools of treatment combinations of various sizes, in **Fig. 47** through **Fig. 50**.

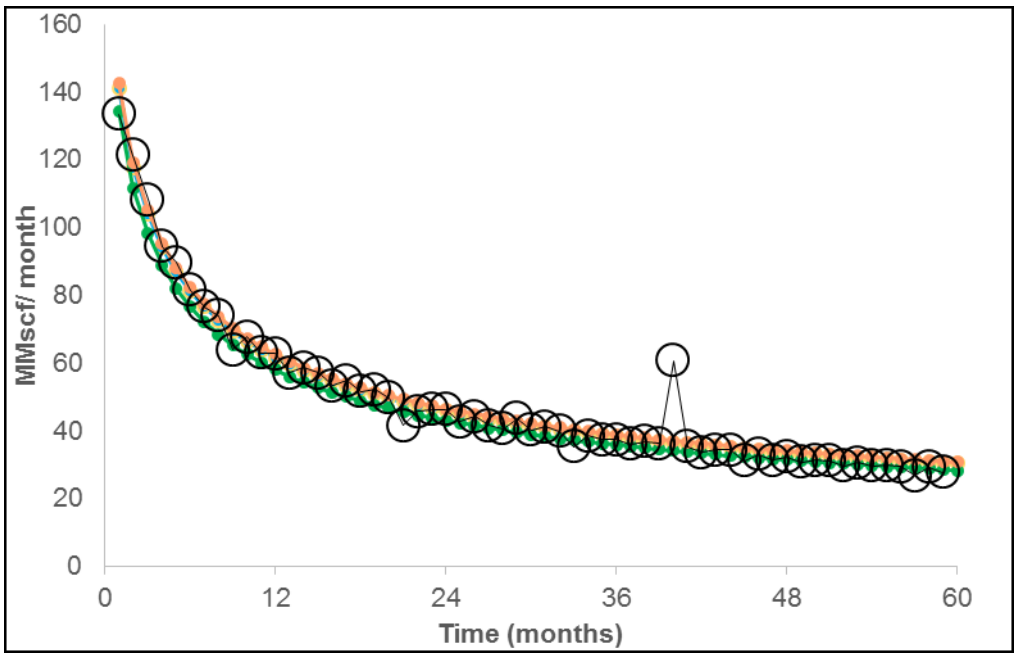

Fig. 47—Well D Probabilistic forecasts: 12-month history match, identified from 1,000 DOE runs

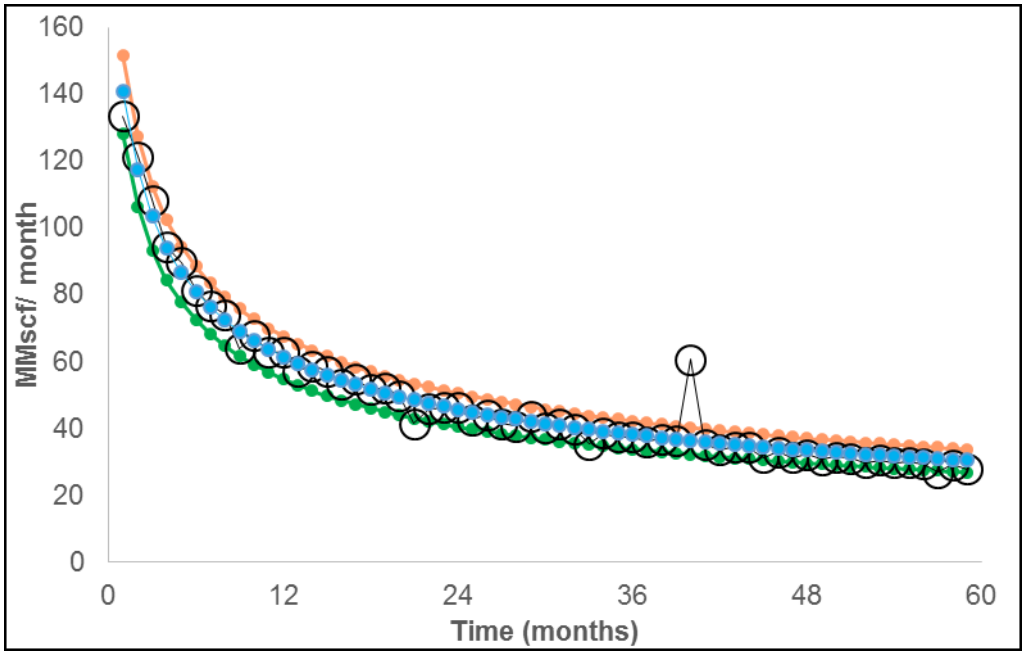

Fig. 48— Well D Probabilistic forecasts: 12-month history match, identified from 250 DOE runs

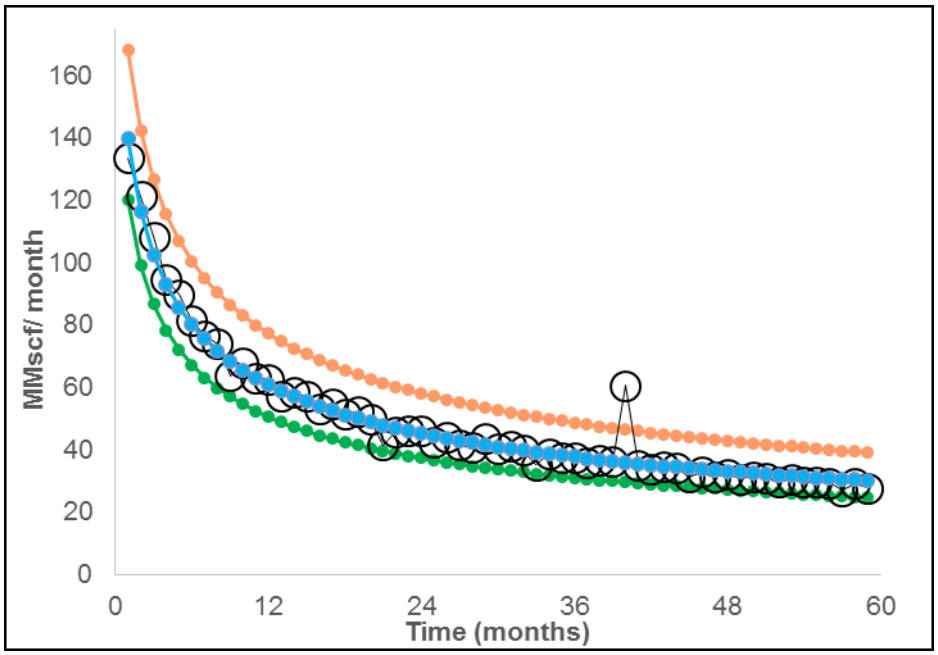

Fig. 49—Well D Probabilistic forecasts: 12-month history match, identified from 125 DOE runs

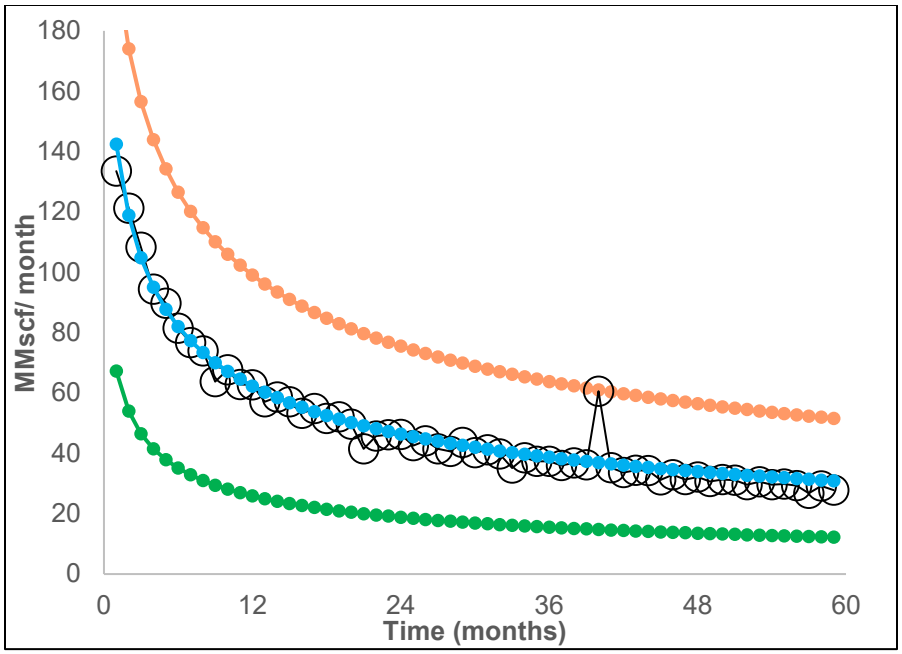

Fig. 50—Well D Probabilistic forecasts: 12-month history match, identified from 45 DOE runs

We compare the P10/P90 ratios of the forecasts shown in Fig. 47 through Fig. 50 in **Table 10**.

Table 10—Effect of # DOE runs on Probabilistic Forecasts and P10/P90 ratio

DOE Runs	P10/P90 ratio			
	q, 12 months	q, 60 months	Q, 12 months	Q, 60 months
1000	1.08	1.09	1.07	1.08
250	1.23	1.25	1.20	1.23
125	1.53	1.58	1.41	1.51
45	3.83	4.21	3.25	3.74

From Table 10, we can see that when probabilistic forecasts are identified from a decreased number of best-matched treatment combinations, that our ranges (and

subsequent P10/P90 ratios) become larger. While we could conclude that narrow probabilistic ranges may be adequate when forecasting a single well (assuming no brash changes to production), we conclude that slightly wider ranges may be more appropriate for modest planning purposes, or when evaluating a larger set of wells with greater reservoir and completion variability.

Identifying probabilistic forecasts from enlarged ranges could suggest the workflow we present could be used to probabilistically estimate resources volumes: when there is no “real” set of production data which to history “match”, our ranges should be wider, and obtaining "matches" from a less populated design space helps us achieve that.

3.1.7 Comparing DOE-generated forecasts with forecasts generated with software

In this section, we validate capabilities of our workflow with the RTA production forecasting capabilities of IHS Harmony. Harmony is a popular industry software in industry, and is considered to be robust by the oil and gas community. We will use known well data, as well as portions of the DOE treatment combinations which yielded the seven best-fit history-matches and subsequent forecasts (for Well D) in Section 3.1.1 in this portion of work.

We begin by generating production forecasts with Harmony using known parameters of Well D, (shown in **Table 11**) and the reservoir and completion data of each of the best-fit treatment combinations (shown in **Table 12**).

Table 11— Known well parameters, required for forecasting with RTA in Harmony, Well D

Well	Temperature, °F	n_f	TVD (ft.)	Reservoir pressure (psi)	Lateral length (ft.)
D	220	8	7953	3698	3084

The seven treatment combinations which yielded the seven best-fit history-matches for Well D, are also reviewed in Table 12.

Table 12— Treatment combinations which yield the best-fit history matches: Well D, 12-month history match

Run	φ	h	x_f	k
880	0.065	375	250	250
682	0.06	250	250	600
941	0.065	200	300	600
447	0.055	325	200	600
108	0.05	300	350	250
119	0.05	350	300	250
1167	0.07	350	200	400

We then compare each of the best-fit forecasts of Well D (generated using our methods and the treatment combinations listed in Table 12), to the corresponding forecast generated in Harmony (using the same input parameters of that treatment combination), and assess how the forecasts generated using either method compare to the true production of Well D. We compare three pairs of forecasts, as well as the true production of Well D, in **Fig. 51** through **Fig. 53**. The three pairs of forecasts shown here were chosen at random, the remaining four pairs of forecasts—generated using the

four remaining treatment combinations highlighted in Table 12—are shown in **Fig. 59** through **Fig. 62**, in the Appendix.

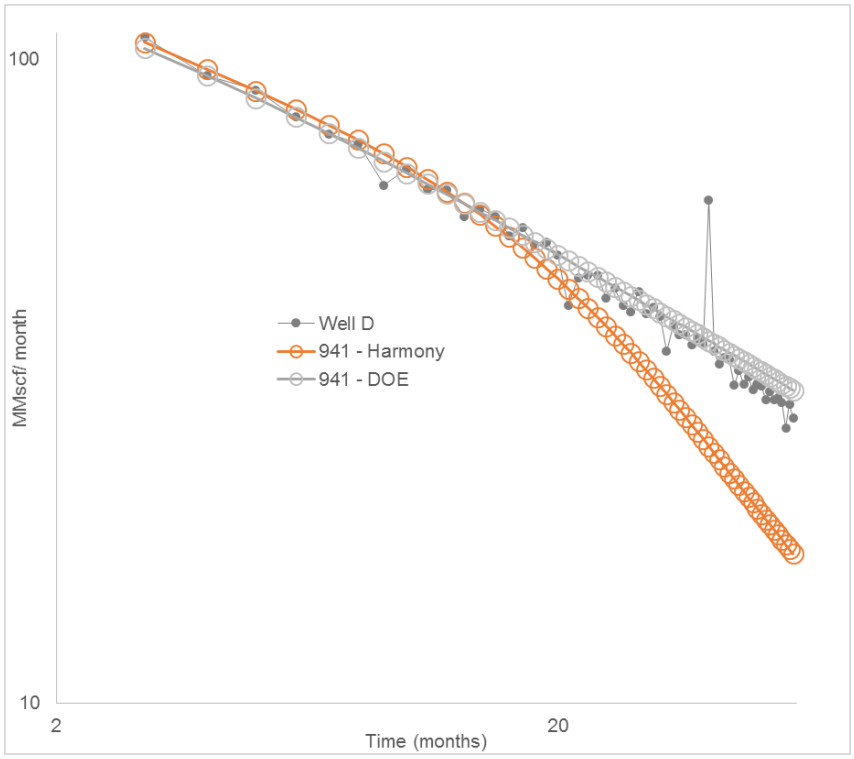

Fig. 51— Comparing Harmony vs. DOE method forecasts, Run 941

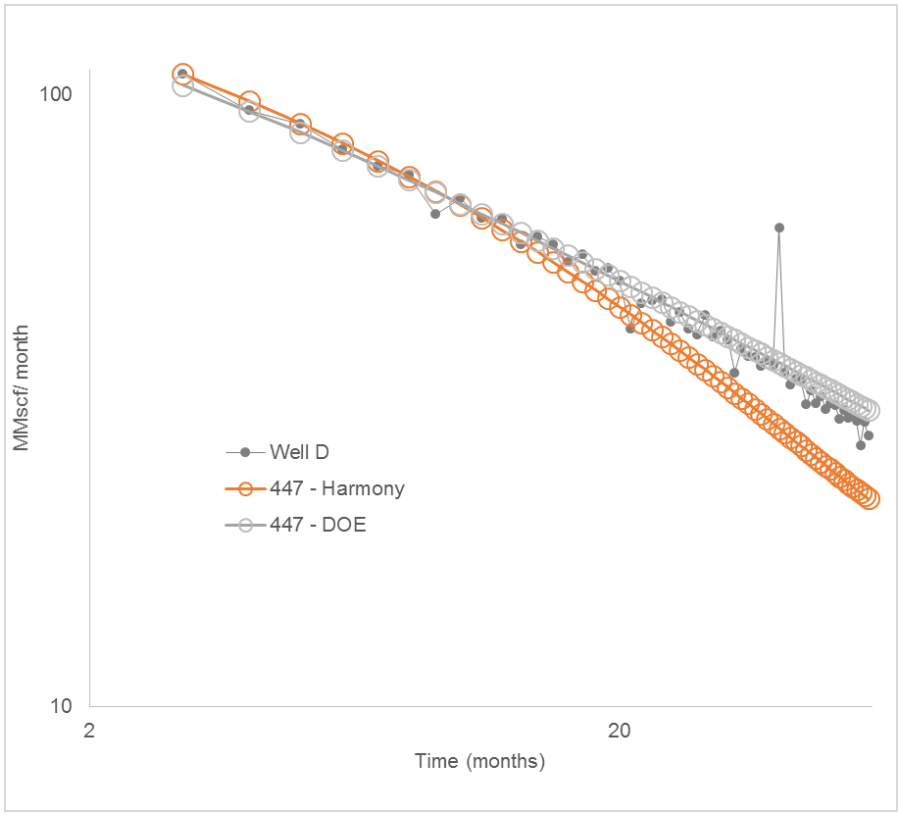

Fig. 52— Comparing Harmony vs. DOE method forecasts, Run 447

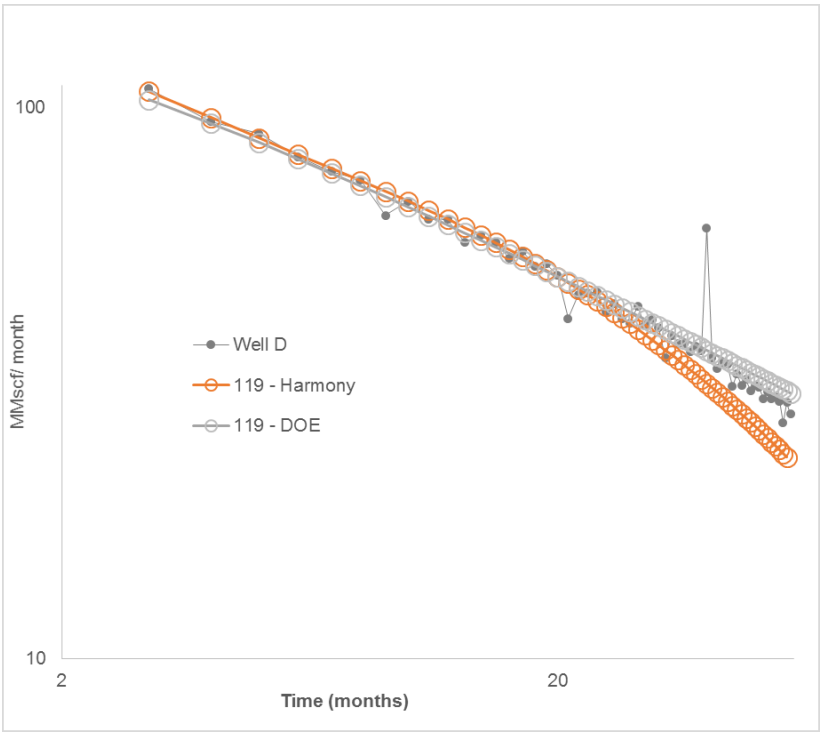

Fig. 53— Comparing Harmony vs. DOE method forecasts, Run 119

From Fig. 51 through Fig. 53, we can see that the forecasts generated with Harmony, compared to the corresponding forecast generated using our DOE methods, visually agree, although tend to diverge over time. It can also be seen from these figures that forecasts generated with our proposed methods visually match the true production of Well D more closely than forecasts generated (using the same input parameters) with Harmony. The pairs of forecasts shown in the Appendix follow this same trend.

We show the discrepancies between the each of the three forecasts in each figure (Fig. 51 through Fig. 53, as well as Fig. 59 and Fig. 62**)**, in **Table 13**.

Table 13— Comparing 60-month EURs, DOE and Harmony forecasts, Well D

	60-month EUR (MMscf)		Discrepancy (Well D, 60-month EUR 2893 MMscf)	
Run	**DOE**	**Harmony**	**DOE**	**Harmony**
880	2962	2654	2.38%	-8.26%
682	2942	2479	1.69%	-14.32%
941	2940	2541	1.62%	-12.18%
447	2931	2639	1.31%	-8.79%
108	2916	2807	0.80%	-2.98%
119	2916	2774	0.80%	-4.13%
1167	2911	2722	0.61%	-5.92%

While this portion of work was only performed with one well, we have reason to believe from other recent work done in industry that the results we see is not anomalous: when testing the RTA production forecasting capabilities of Harmony for oil production, Moinfar and Erdle (2016) encountered similar underestimations in cumulative production, attributing these lower-than-expected cumulative production estimates to the software's inability to capture all physics associated with their assumptions, and in turn, over-compensating for those missing physics by "significantly degrading" fracture properties when history-matching historical data (Moinfar, Erdle 2016).

3.2 Incorporating Economic Constraints to Forecasts

Another advantage of history-matching and forecasting production with our methods is that only a software such as Microsoft Excel is required: in a single Microsoft Excel file, the user has the freedom to customize the interface of the program used to history-match (and generate forecasts), and the freedom to history-match on the

basis of any parameter (Harmony is also limited in this regard as only a few parameters can be "automatically estimated" with the APE tool). We have mentioned in previous sections that a shortcoming of Harmony is that it does not allow the user to specify any economic variables in a forecast. However, with Excel, the user has the ability to incorporate economic parameters such as working interest, royalties, lease operating expense (LOE), and commodity price, to "end" a forecast once an economic limit is reached.

We use **Eq. 15** (Mian, 2011) to calculate the minimum rate at which gas must be produced per month to remain economic (EL_{gas}) for forecasts within this section.

$$EL_{gas} = \frac{WI \times LOE \times (1 + IRR)}{(1 - t) \times NRI \times P_{gas}} \quad \ldots\ldots\ldots\ldots\ldots\ldots\ldots\ldots\ldots\ldots\ldots\ldots \quad (15)$$

We assume:

- Working interest (WI) of 100%
- Lease operating expense (LOE) of $2500 per well, per month
- Internal rate of return (IRR) of 15%
- Tax rate (t) of 7.5%
- Net revenue interest (NRI) of 100%
- Gas price of $3/ MMBtu
- 1 MMBtu = 1 Mscf = .001 MMscf

These values yield an EL_{gas} ≈1 MMscf/ month (see **Table 14**).

Table 14—Economic Limit assumptions and calculations

WI	100	%
IRR	15	%
t	7.5	%
NRI	100	%
LOE	$ 2,500.00	$/ well/ month
Gas price	$ 3.00	$/ MMBtu
Gas price	$ 3,000.00	$/ MMscf
EL_gas	1.04	MMscf/ month

Although not all forecasts generated in this work would have necessarily been affected by an economic limit, performing evaluations prior to incorporating economics could strongly affect the evaluation of the probabilistic range of forecasts. Incorporating economic limits can be much more complex than what we have demonstrated here, as we hold commodity price flat throughout the forecast (rather than use escalating or otherwise variable prices), we hold LOE flat, nor do we incorporate variables such as inflation.

We suspect that had more complex economics been incorporated into the production forecasting analysis here, that impacts to longer-term production forecasts would have been realized, and recommend that when generating longer-term production forecasts and determining probabilistic forecasts and estimates, that these economic factors be considered.

3.3 Results Summary

We have found that using DOE techniques are reliable in the history-matching process, and in generating a range of forecasts that match "future" production satisfactorily (as long as reliable probability distributions of input parameters are satisfactorily known). We have also discussed that incorporating D-Optimal designs are helpful when "randomly" creating experimental runs, when the effects of certain input parameters vary discretely and definitively (when decimal change to parameters such as lateral lengths and number of fractures tend to be negligible).

We have demonstrated in this work that DOE techniques (specifically, D-Optimal designs) can be seamlessly incorporated to reduce the time required to obtain many satisfactory history-matches (in this work, we identified up to 40 best matches per well), and to generate appropriate and satisfactory production forecasts with RTA, even when production data is limited. From these best-fitting forecasts, appropriate P10, P50, and P90 forecasts can be elected.

We showed that DOE techniques can be used in place of MCS to generate *thousands* of possible treatment combinations in a matter of seconds, and showed that by ranking m_{cp}—a product of each treatment combination—the select treatment combinations which will yield the best-fit forecasts—during transient flow—can be very quickly identified, at the click of a button. We showed how independent methods to forecast production in BDF can be integrated with the workflow to forecast production beyond transient linear flow.

.

4. SUMMARY AND CONCLUSIONS

In this work, we have discussed that there is currently a lack of practical methods to systematically, probabilistically forecast production in unconventional, undeveloped plays using Rate Transient Analysis (RTA). While numerical simulation techniques can be used to forecast production in unconventional plays, they are time-consuming, costly, and come with a steep learning curve, making them less attractive to a wide audience. Additionally, when generating many forecasts (to create a probabilistic range of forecasts), numerical simulation techniques become exponentially more burdensome.

We also discussed that empirically-based production forecasting solutions, in combination with Monte Carlo Simulation (MCS) techniques, can be used to build a range of probabilistic forecasts, however empirical solutions are not as robust as other methods, as they do not require the input of physical reservoir or completion parameters of the well for analysis.

Production forecasting with RTA, however, is considered to be more robust than empirical production forecasting techniques, in that it captures the physics of the reservoir and the completion characteristics of the well, yet is much simpler than numerical simulation techniques in application. While MCS can be incorporated into the process of forecasting production with RTA, it is sub-optimal when trying to history match available production data due to the challenge of non-unique solutions associated with RTA: many of the matches MCS generates may yield redundant results.

In this work, we have presented methods which show that probabilistically forecasting production with RTA—during transient flow—can be made more efficient by incorporating Experimental Design—or Design of Experiment (DOE)—techniques. We have shown that DOE techniques can generate appropriate, pre-designed treatment combinations which yield satisfactory—and unique—history matches, even when available production data is limited, and that these unique treatment combinations can be identified in seconds. These treatment combinations can be used to generate forecasts, in conjunction with any software which allows for production forecasting with RTA, to create a range of forecasts, from which probabilistic forecasts could be extracted.

We have shown that by incorporating DOE techniques into probabilistic production forecasting analyses, the number of forecasts which need to be generated, necessary to build a reliable range of results, can be significantly reduced: while MCS techniques require thousands of runs be performed, we are able to extract P10, P50, and P90 forecasts from a much smaller number of forecasts (no more than 50, in this work).

We also showed an alternative method to generate many forecasts at once—more quickly than in an RTA software—using the treatment combinations of RTA input parameters created with DOE, to history-match available production data. While this method is very simplified, we showcased for several MFHWs in the Barnett Shale that the method can sufficiently history-match and generate valid production forecasts that are in agreement with the true "future" production of the wells presented while in transient linear flow. We also propose methods which incorporate Arps' decline methods to forecast production once the well has reached BDF.

4.1 Conclusions

In this work we conclude that:

- DOE techniques, in combination with RTA, can be used to efficiently history match, and forecast production for, MFHWs currently producing from the Barnett Shale. The process of forecasting production from those history matches can be performed, as we have shown, in a simple Excel spreadsheet, or can be performed by, and/or validated with, any currently available software which allows for production forecasting with RTA.
- Using a simple Excel spreadsheet, rather than an RTA software program, to forecast allows for the input of economic parameters such as current gas price, lifting costs to "stop" production once the well is no longer able to produce economically. These same (simple) features are not currently available in software which generate production forecasts with RTA.
- By using DOE techniques in lieu of MCS, the number of combinations of input parameters which yield redundant forecasts and results, are minimized, reducing the total number of forecasts which need to be generated to compile a valid and reliable range of results. From this range, individual P10, P50, and P90 forecasts can be extracted, required for PRMS resource inventories.

REFERENCES

Anderson, D. M., Liang, P., & Okouma Mangha, V. (2012, January 1). Probabilistic Forecasting of Unconventional Resources Using Rate Transient Analysis: Case Studies. Society of Petroleum Engineers. doi:10.2118/155737-MS

Arps, J. J. (1945, December 1). Analysis of Decline Curves. Society of Petroleum Engineers. doi:10.2118/945228-G

Browning, J & Tinker, Scott & Ikonnikova, Svetlana & Gülen, Gürcan & Potter, E & Fu, Qilong & Horvath, S & Patzek, Tad & Male, Frank & Fisher, W.L. & Roberts, Forrest & Medlock, Kenneth. (2013). Barnett Shale Model - 1: Study develops decline analysis, geologic parameters for reserves, production forecast. Oil & Gas Journal. 111. 63-71.

Capen, E. C. (1976, August 1). The Difficulty of Assessing Uncertainty (includes associated papers 6422 and 6423 and 6424 and 6425). Society of Petroleum Engineers. doi:10.2118/5579-PA

Cherian, B. V., Fields, K. W., Crissman, S. C., Itibrout, T., & Yates, M. E. (2009, January 1). Maximizing Effective Fracture Half-Length to Influence Well Spacing. Society of Petroleum Engineers. doi:10.2118/122514-MS

Ezisi, I., Hale, B. W., Watson, M. C., & Heinze, L. (2012, January 1). Assessment of Probabilistic Parameters for Barnett Shale Recoverable Volumes. Society of Petroleum Engineers. doi:10.2118/162915-MS

Fekete. http://www.fekete.com/SAN/WebHelp/FeketeHarmony/Harmony_WebHelp/Content/HTML_Files/Reference_Material/Analysis_Method_Theory/Unconventional_Reservoir_Theory.htm. (Accessed June 2018).

Fetkovich, M. J., Fetkovich, E. J., & Fetkovich, M. D. (1996, February 1). Useful Concepts for Decline Curve Forecasting, Reserve Estimation, and Analysis. Society of Petroleum Engineers. doi:10.2118/28628-PA

Fu, Qilong & C. Horvath, Susan & C. Potter, Eric & Roberts, Forrest & Tinker, Scott & Ikonnikova, Svetlana & Fisher, W.L. & Yan, Jihua. (2015). Log-derived thickness and porosity of the Barnett Shale, Fort Worth basin, Texas: Implications for assessment of gas shale resources. AAPG Bulletin. 99. 119-141. 10.1306/07171413018.

Information Technology Laboratory (ITL), the National Institute of Standards and Technology (NIST). www.itl.nist.gov/div898/handbook/pri/section5/pri521.htm (accessed March 2018- July 2018).

Lee, W. J., & Sidle, R. E. (2010, January 1). Gas Reserves Estimation in Resource Plays. Society of Petroleum Engineers. doi:10.2118/130102-MS

McVay, D. (2015, February 1). Industry Needs Re-Education in Uncertainty Assessment. Society of Petroleum Engineers. doi:10.2118/0215-0072-JPT

Mian, M.A. Project Economics and Decision Analysis. Tulsa, OK: PenWell, 2011.

Petrowiki. https://petrowiki.org/Gas_formation_volume_factor_and_density. (Accessed June 2018).

University of Louisiana at Lafayette. booksite.elsevier.com/9780750682701/solutions/PseudoPressure.xls. (Accessed March 2018- July 2018).

Wattenbarger, R. A., El-Banbi, A. H., Villegas, M. E., & Maggard, J. B. (1998, January 1). Production Analysis of Linear Flow Into Fractured Tight Gas Wells. Society of Petroleum Engineers. doi:10.2118/39931-MS

Yu, W., & Sepehrnoori, K. (2013, March 23). Optimization of Multiple Hydraulically Fractured Horizontal Wells in Unconventional Gas Reservoirs. Society of Petroleum Engineers. doi:10.2118/164509-MS

Table 15—Key of Barnett Shale MFHWs well aliases

Well alias	API (last four digits)
A	-3840
B	-3418
C	-4020
D	-4202
E	-3869
F	-3367
G	-4210
H	-3895
I	-3878
J	-3676
K	-3930

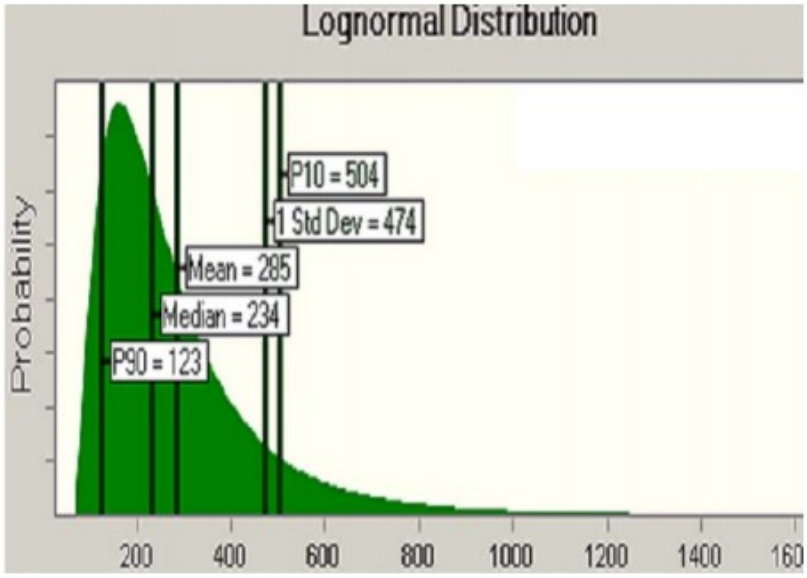

Fig. 54—Fracture half-length probability distribution (Cherian)

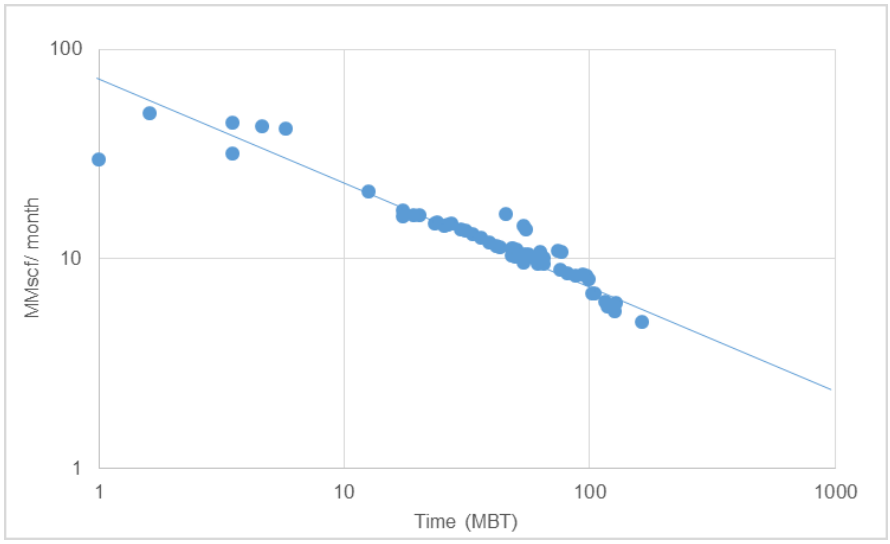

Fig. 55—Log-log plot, Well F

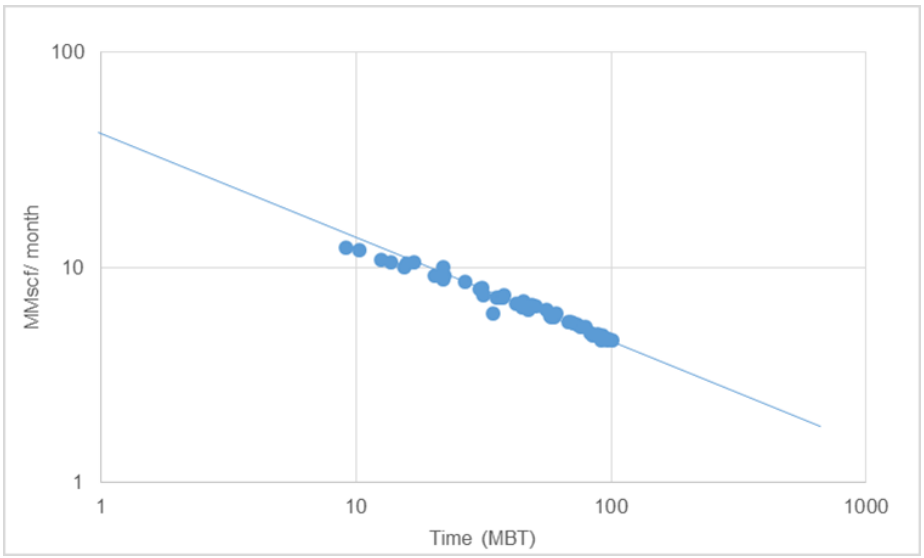

Fig. 56—Log-log plot, Well H

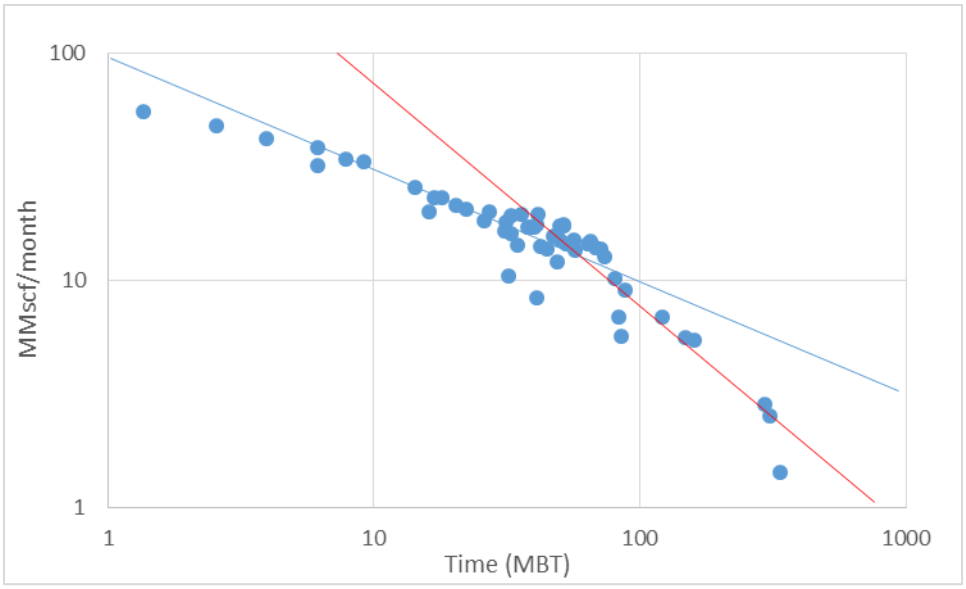

Fig. 57—Log-log plot, Well I

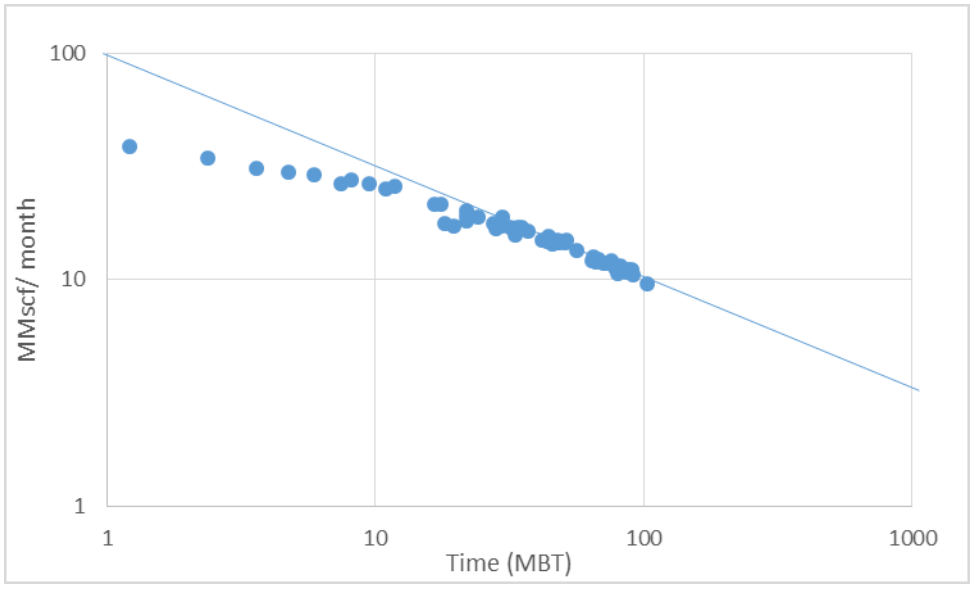

Fig. 58—Log-log plot, Well J

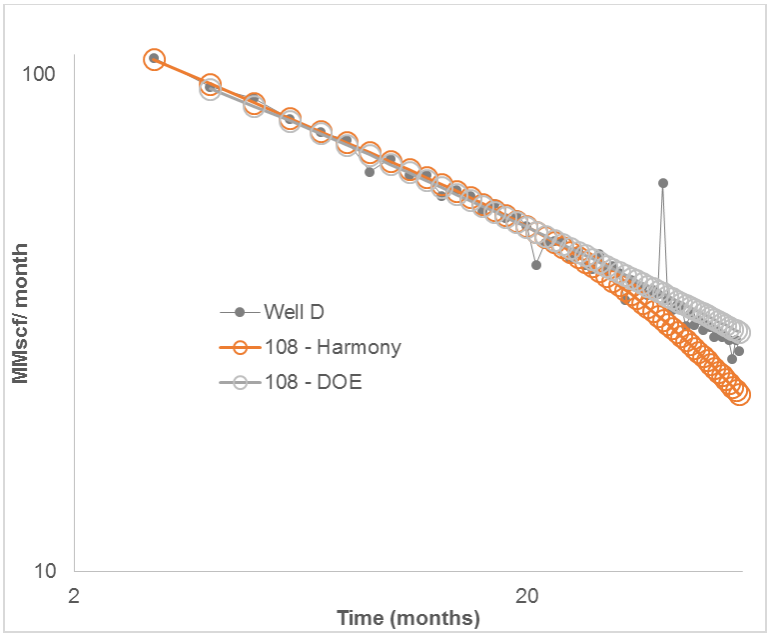

Fig. 59—Comparing Harmony vs. DOE method forecasts, Run 108

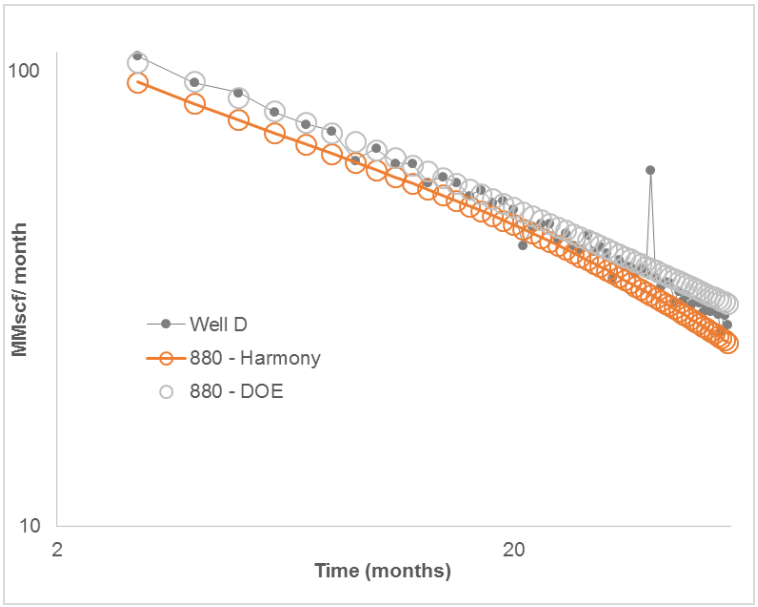

Fig. 60—Comparing Harmony vs. DOE method forecasts, Run 880

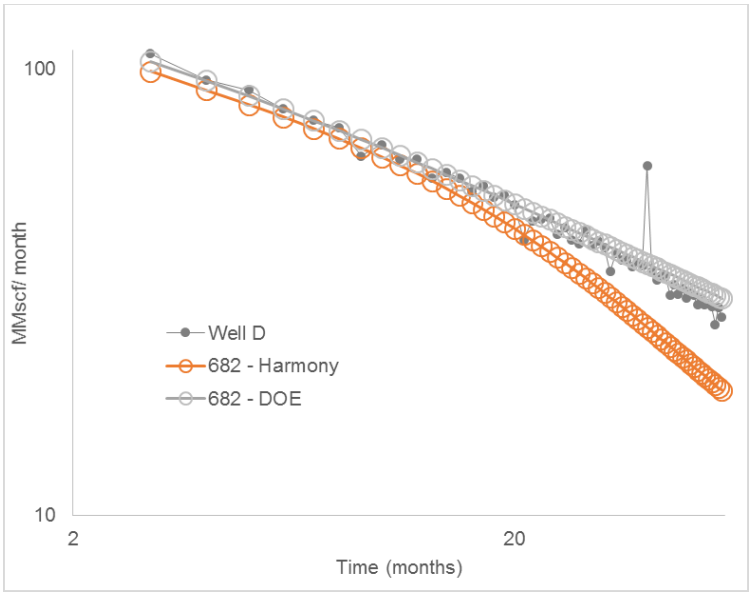

Fig. 61—Comparing Harmony vs. DOE method forecasts, Run 682

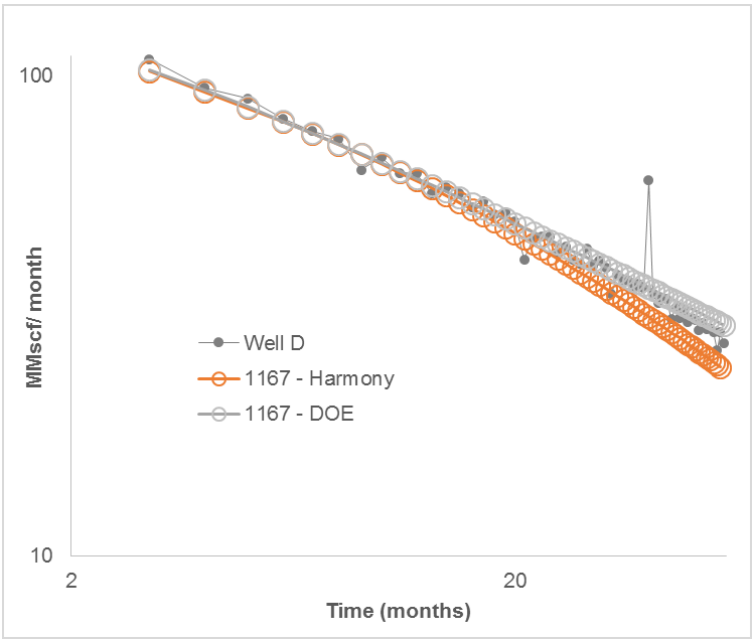

Fig. 62—Comparing Harmony vs. DOE method forecasts, Run 1167